ALGORITHMS AND PROTOCOLS FOR EFFICIENT MULTICAST, TRANSPORT, AND CONGESTION CONTROL IN WIRELESS NETWORKS

BY

KAI SU

A dissertation submitted to the

Graduate School—New Brunswick

Rutgers, The State University of New Jersey

In partial fulfillment of the requirements

For the degree of

Doctor of Philosophy

Graduate Program in Electrical and Computer Engineering

Written under the direction of

Dipankar Raychaudhuri and Narayan B. Mandayam

And approved by

_____

_____

_____

_____

New Brunswick, New Jersey

October, 2016

ABSTRACT OF THE DISSERTATION

Algorithms and Protocols for Efficient Multicast, Transport, and Congestion Control in Wireless Networks

By KAI SU

Dissertation Directors:
Dipankar Raychaudhuri and Narayan B. Mandayam

Effective and efficient support for wireless data transfer is an essential requirement for future Internet design, as the number of wireless network users and devices, and the amount of traffic flowing through these devices have been steadily growing. This dissertation tackles several problems, and proposes algorithmic and protocol design solutions to better provide such support. The first problem is regarding the inefficiency of multicast in wireless networks: a transmission is considered a unicast despite the fact that multiple nearby nodes can receive the transmitted packet. Random network coding (RNC) is considered a cure for this problem, but related wireless network radio resources, such as transmit power, need to be optimally allocated to use RNC to its full advantage. A dynamic radio resource allocation framework for RNC is proposed to maximize multicast throughput. Its efficacy is evaluated through both numerical and event driven simulations.

Next, we present the design of MFTP, a clean-slate transport protocol aimed for supporting efficient wireless and mobile content delivery. Current transport protocol of the Internet, TCP, is known to fall short if the end-to-end path involves wireless links

where link quality varies drastically, or if the client is mobile. Building on a mobility-centric future Internet architecture, MobilityFirst (MF), a set of transport protocol components are designed to collectively provide robust and efficient data transfer to wireless, or mobile end hosts. These include en-route storage for disconnection, in-network transport service, and hop-by-hop delivery of large chunks of data. A research prototype is built and deployed on ORBIT testbed to evaluate the design. Results from several wireless network use case evaluations, such as large file transfer, web content retrieval, and disconnection services, have shown that the proposed mechanisms achieve significant performance improvement over TCP.

Finally, a scalable, network-assisted congestion control algorithm is proposed for the MobilityFirst future Internet architecture. In MobilityFirst, various intelligent functionalities, such as reliability and storage, are placed inside the network to assist with data delivery. Traditional end-to-end congestion control such as that carried out by TCP becomes unsuitable as it is unable to take advantage of such in-network functionalities. We design a congestion control policy that uses explicit congestion notifications from network routers and rate control at traffic sources. The hop-by-hop reliability provided in MF simplifies end-to-end reliable delivery of wireless/mobile data, but often requires routers to keep per-flow queues to carry out congestion control which could become impractical in the presence of a large number of flows. Our approach builds on a per-interface queueing scheme, and we show through simulation that it is able to substantially improve delay, fairness, and scalability with only $\leq 6\%$ link utilization degradation, compared with a per-flow queueing based scheme.

Acknowledgements

I would like to express my deepest gratitude to my advisors, Prof. Dipankar Raychaudhuri and Prof. Narayan B. Mandayam, for their continuous support and guidance. Prof. Ray's acute technological vision and strong passion for revolutionizing the Internet have greatly enlightened and inspired me. The wisdom in his advice, on research and life, has guided and will continue to guide me through the challenges ahead. Prof. Mandayam has cultivated my skill of modeling abstract problems mathematically, and it has benefitted me tremendously throughout my Ph.D. study. His rigor, accuracy, and professionalism are something that I strive to attain as a researcher and engineer. I am deeply indebted to them for being my Ph.D. dissertation advisors.

I am honored to have the opportunity to be mentored by and to work with Prof. K. K. Ramakrishnan on MFTP design and its congestion control in particular. I admire him for his expertise, enthusiasm and wholeheartedness. Prof. Ramakrishnan's sharp attention to details has motivated me to be meticulous, to be thorough, and to be able to question and challenge. I can never thank him enough for his mentorship.

I am grateful to Prof. Roy Yates and Prof. Wade Trappe for serving on my dissertation committee and proposal defense committee, respectively. I would also like to thank Ivan Seskar for his constant support on various aspects of practical experimentation on the ORBIT testbed.

I enjoyed collaborating with Dr. Dan Zhang, Francesco Bronzino, and Shreyasee Mukherjee and am grateful to them for their time and efforts. I am lucky to meet and become friends with many other students at WINLAB.

Last but not the least, I want to thank my parents, Chunxiang Su and Qiong Yu, and my fiancee, Wenjie Li, for their perpetual faith, encouragement, and love.

Dedication

To *Chunxiang Su*, *Qiong Yu*, and *Wenjie Li*

Table of Contents

Abstract ii

Acknowledgements iv

Dedication v

1. Introduction 1

1.1. Motivation for wireless network algorithm and protocol design 1

1.2. Outline of the remainder of the dissertation and key contributions . . . 3

1.2.1. Dynamic Resource Allocation for Random Network Coding (Chapter 2) 3

1.2.2. MFTP: Transport protocols for MobilityFirst future Internet architecture (Chapter 3) 4

1.2.3. Scalable, network-assisted congestion control for the MobilityFirst future Internet architecture (Chapter 4) 5

2. Dynamic Resource Allocation for Random Network Coding 6

2.1. Introduction 6

2.2. Preliminaries 10

2.2.1. Differential Equation Framework for RNC 10

2.3. Resource Allocation Algorithm for Wireless Network Coding 14

2.3.1. Problem Formulation 14

2.3.2. Gradient-based Resource Allocation Algorithm 15

2.3.3. Relationship to existing literature on resource allocation for RNC 17

2.4. Dynamic Power Control in RNC 18

2.4.1. Interference Model 18

2.4.2. Centralized Power Control 19

2.4.3. Online Power Control 21
Motivation for online power control algorithm 21
Deriving the online algorithm 21
Discussion regarding implementation considerations. 24
2.4.4. Numerical Results 26
Centralized algorithm 26
Comparison between DE-based centralized algorithm and flow-based algorithm 28
Online algorithm 29
2.5. Dynamic CSMA Mean Backoff Delay Control in RNC 30
2.5.1. CSMA Model 31
2.5.2. Centralized Gradient Algorithm for CSMA Mean Backoff Delay Control 33
2.5.3. Online Gradient Algorithm for CSMA Mean Backoff Delay Control 34
2.5.4. Numerical Results 35
Centralized algorithm 36
Online algorithm 36

3. Transport protocols for MobilityFirst future Internet architecture . 39
3.1. Introduction 39
3.2. Requirements for transport layer service for ICN 41
3.3. MFTP design 44
3.3.1. Segmentation and re-sequencing 45
3.3.2. Coordinated End-to-end error recovery and hop-by-hop reliable delivery 46
3.3.3. In-network transport proxy 48
3.3.4. Flow control and congestion control 50
3.3.5. Multicast 52
3.4. Implementation 53

3.5. Case studies and evaluations 55
3.5.1. Large content delivery over wireless 56
3.5.2. Transport proxy for disconnection 58
Comparison between network-proactive and receiver-driven approaches 59
3.5.3. Web content retrieval 60
3.6. Related work 62

4. Scalable, network-assisted congestion control for the MobilityFirst future Internet architecture 64
4.1. Introduction 64
4.2. Background on MobilityFirst and data transport in MF 67
4.2.1. MobilityFirst architecture overview 67
4.2.2. Data transport in MF 68
4.3. Design Considerations 68
4.3.1. Back-pressure 69
4.3.2. Fair share allocation 69
4.3.3. Router queue build-up 70
4.4. Design 70
4.4.1. Overall framework 70
4.4.2. Local fair share estimation 71
4.4.3. Rate adjustment 72
Frequency of control 72
Control logic 72
4.4.4. Aggressive bootstrapping 74
4.5. Evaluation 74
4.5.1. Simulator 74
4.5.2. Single bottleneck scenario 75

Understanding cause of per-interface queueing throughput impairment 76
4.5.3. RocketFuel topologies 76
4.6. Related work 81

5. Concluding remarks 83

References 85

Chapter 1

Introduction

1.1 Motivation for wireless network algorithm and protocol design

The past decade sees several prominent trends of evolution of the Internet. The number of devices connected to the Internet through wireless technologies has been rapidly and steadily growing. Not only smart phones, but other handheld devices, such as tablets, and ebook readers, become the new "norm" of communication with the Internet. Along with the popularity of wirelessly connected handheld devices, wireless traffic has been surging during the last couple of years and it is still continuing. Improved communication capacity and availability of wireless access points are poised to cater to the end users' appetite for different kinds of contents, such as web pages, photos, and even videos.

Multiple layers of the networking stack need to continuously evolve to adapt to the ubiquity of wireless-based networking, the ever-increasing wireless traffic demand, and emerging mobile data delivery service patterns. Take PHY and MAC layers from the networking protocol stack for an example. Novel PHY technologies, and efficient PHY/MAC resource management algorithms are demanded to sustain high data rate and wireless channel utilization. Consider also the network and transport layers. In the current Internet architecture, end points of data transport are statically bound with IP addresses, which are used both as identity and locator. This results in difficulty and inefficiency in supporting seamless data transfer to a mobile end point. Because both the identity and location would change when it moves, and connection to the same end point needs to be re-established. Thus mobility support should be factored into the network and transport layer design.

This dissertation aims to address several existing problems of wireless networks: i) we design radio resource allocation algorithms for random network coding, to support efficient multicast in wireless networks; ii) we design and validate a suite of transport protocols, on top of the MobilityFirst future Internet architecture, to handle client disconnection and mobility in mobile content deliveries; iii) we propose explicit congestion notification based congestion control algorithms for hop-by-hop data transfers, which are suitable for wireless connections. The general goal of all these projects is to improve efficiency and scalability of wireless networking, through meticulous algorithmic and protocol design. We discuss their individual motivations in the following.

The first problem is regarding the intrinsic inefficiency in the wireless broadcast medium. Consider a WiFi network. In a single collision domain, every node can hear other nodes' transmission, and each transmission is effectively a broadcast in this domain. Therefore such wireless networks can potentially support multicast. Unfortunately, due to the lossy nature of wireless links, reliable multicast has to rely on unicast-based retransmissions, resulting in under-utilized broadcast channel. An emerging transport paradigm, Random Network Coding (RNC) addresses this problem. RNC allows transmitting nodes to randomly combine packets, and makes each transmitted packet potentially useful to multiple other nodes. Of paramount importance for this kind of system to operate to its full advantage is the optimized allocation of wireless network resources, such as transmit power and transmission aggressiveness. To this end, a mathematical framework of radio resource management is developed in this dissertation, to guide RNC to optimize the raw throughput of the wireless medium.

The second problem concerns about lack of efficient transport protocol support for mobile content retrieval. Current transport protocol of the Internet, TCP, is known to perform poorly if the end-to-end path involves wireless links where link quality varies significantly and randomly over time. In addition, TCP binds a connection to the two endpoints' network addresses. When one endpoint moves and changes its point of attachment, the connection is disrupted and has to be reestablished, resulting in interrupted transfers and prolonged response times. Building on a mobility-centric future Internet architecture, a set of transport protocols are designed in this dissertation

to provide robust and efficient data transfer to wireless, or mobile end hosts.

The third problem we examine is on congestion management. Hop-by-hop reliable transfer of large chunks are considered more efficient in wireless networks, and are adopted in MobilityFirst to provide in-network reliability. Previous works on hop-by-hop transfer utilize back pressure based congestion control mechanisms, and presume that each router maintains per-flow queues in its memory. Such a queueing model, combined with certain fair scheduling policies, such as Round Robin, achieves good throughput, delay, and fairness simultaneously. Nevertheless, with an enormous number of concurrent, in-transit flows, such per-flow queueing based schemes incur a non-negligible amount of cost in terms of memory consumption, and computation complexity. In this dissertation, we attempt to design scalable congestion control mechanisms, with a much simplified queueing model, i.e. per-interface queueing, to attain similar performance as per-flow queueing.

1.2 Outline of the remainder of the dissertation and key contributions

1.2.1 Dynamic Resource Allocation for Random Network Coding (Chapter 2)

By means of a differential equation framework which models RNC throughput in terms of lower layer parameters, we propose a gradient based approach that can dynamically allocate MAC and PHY layer resources with the goal of maximizing the minimum network coding throughput among all the destination nodes in a RNC multicast. We exemplify this general approach with two resource allocation problems: (i) power control to improve network coding throughput, and (ii) CSMA mean backoff delay control to improve network coding throughput. We design both centralized algorithms and online algorithms for power control and CSMA backoff control. Our evaluations, including numerically solving the differential equations in the centralized algorithm and an event-driven simulation for the online algorithm, show that such gradient based dynamic resource allocation yields significant throughput improvement of the destination nodes in RNC. Further, our numerical results reveal that network coding aware power control

can regain the broadcast advantage of wireless transmissions to improve the throughput.

1.2.2 MFTP: Transport protocols for MobilityFirst future Internet architecture (Chapter 3)

This chapter presents the design and evaluation of clean-slate transport layer protocols for the MobilityFirst (MF) future Internet architecture based on the concept of named objects. The MF architecture is a specific realization of the emerging class of Information Centric Networks (ICN) that are designed to support new modes of communication based on names of information objects rather than their network addresses or locators. ICN architectures including MF are characterized by the following distinctive features: (a) use of names to identify sources and sinks of information; (b) storage of information at routers within the network in order to support content caching and disconnection; (c) multicasting and anycasting as integral network services; and in the MF case (d) hop-by-hop reliability protocols between routers in the network. These properties have significant implications for transport layer protocol design since the current Internet transports (TCP and UDP) were designed for the end-to-end Internet principle which uses address based routing with minimal functionality (i.e. no storage or reliability mechanisms) within the network. Several use cases including web access, large file transfer, machine-to-machine and multicast services are considered, leading to an identification of four basic functions needed to constitute a flexible transport protocol for ICN: (i) fragmentation and end-to-end re-sequencing; (ii) lightweight end-to-end error recovery with in-network transport proxies; (iii) optional flow and congestion control mechanisms; and (iv) scalable multicast delivery mechanisms. The design of the MobilityFirst transport protocol (MFTP) framework realizing these features in a modular and flexible manner is presented and discussed. The proposed MFTP protocol is then experimentally evaluated and compared with TCP/IP for a few representative scenarios including mobile data delivery, web content retrieval and disconnected/late binding service. The results show that significant performance gains can be achieved in each case.

1.2.3 Scalable, network-assisted congestion control for the MobilityFirst future Internet architecture (Chapter 4)

Hop-by-hop transfer calls for specialized congestion control mechanisms. This is because with bulk data transfer, congestion detection and control operations have to be carried out on a less granular basis, compared with TCP. This chapter investigates congestion control for hop-by-hop data transfer in MobilityFirst. Theoretically, queuing and scheduling on a per-flow basis achieves the best throughput and fairness across concurrent flows, but with an enormous number of flows, the required resources such as CPU and memory space make such a scheme less attractive. The overall cost of per-flow queues motivates the pursuit of a different congestion control scheme. In this work, we develop aggregated, and scalable mechanisms, which use explicit congestion notification and source rate control, to accomplish similar performance as per-flow queueing based schemes. Preliminary simulation results have shown the proposed schemes only introduce at most 6% degradation of mean link utilization, compared with per-flow queueing. In the meantime, it greatly simplifies queueing and scheduling operations at routers, and substantially improves data transfer performance on additional metrics, such as fairness and delay.

Chapter 2

Dynamic Resource Allocation for Random Network Coding

2.1 Introduction

In wireless networks, resource allocation takes place at multiple layers of the protocol stack. Examples of these include transmit power control, channel allocation, and link scheduling at the PHY/MAC layer and buffer management at the transport layer. While network protocol layering aims to reduce inter-layer dependency and brings noticeable benefits for interconnection, it is recognized that performance can be optimized if network resources at different layers are jointly taken into consideration. Specifically, the PHY and MAC layer resources, which tend to be isolated from upper layer functionalities, can be designed to support performance requirements at routing and transport layers [1]. The resource allocation problem has been extensively studied for different types of wireless networks (see [2–4]), such as cellular networks and wireless ad hoc networks.

Random network coding (RNC) is a new transport paradigm, different from routing and forwarding. It allows the nodes in the network to perform coding of packets at the network layer. It has received a large amount of attention since its inception [5] and has been demonstrated to yield benefits in achieving the optimal network throughput [5], improving network security [6], and supporting distributed storage [7] and content delivery [8]. The topic of resource allocation for RNC has also been visited and existing works include [9–13]. As is known, resource allocation interacts with the performance of wireless networks with a routing-based transport pattern. In fact, the cooperative nature of RNC further complicates this interaction, and varied allocation of resources

at different nodes would lead to unpredictable RNC performance. We will elaborate on this complex interaction using two motivating examples: (i) power control in a wireless network with RNC, and (ii) CSMA backoff control in a wireless network with RNC.

Let us first consider the effects of transmit powers on the performance of random network coding in the wireless network shown in Figure 2.1. The source node, node 1, is trying to multicast to a set of sink nodes, node $\{4, 5, 6\}$. In this network, every node is transmitting and is also able to receive from others. We further assume the network is interference limited, i.e., each transmission is interfered by simultaneous transmissions from other nodes. Therefore, increasing transmit power at a node improves SINR value of its own transmission but raises interference to others. The throughput of the destination nodes thus depend on the power levels at all nodes. To observe this effect, we set the transmit power P_i^{Tx} of each node i to 13dBm at $t = 0$ms. Subsequently, at $t = 500\text{ms}, t = 1000\text{ms}$ and $t = 1500$ms, the transmit powers of node $1, 3, 4$, i.e., $P_1^{\text{Tx}}, P_3^{\text{Tx}}$ and P_4^{Tx} are increased to 14dBm, respectively. As seen in Figure 2.2(a), the power increment of node 1 at 500ms improves the throughput of all the sink nodes, whereas node 3's increment at 1000ms leads to the decrease of throughput of node 4 and 6. Therefore, increasing power at one node does not necessarily improve the throughput at all the destination nodes; on the contrary, it may possibly hurt the throughput at some node.

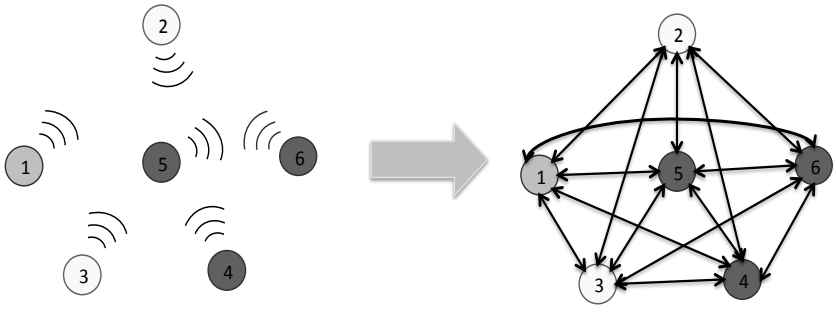

Figure 2.1: Hypergraph model of a wireless network of six nodes with $s = 1$ and $\mathcal{D} = \{4, 5, 6\}$.

Now consider the case of adjusting the backoff time in a CSMA network employing RNC. We consider a network with the same topology as in Figure 2.1 that is utilizing

CSMA as the MAC layer protocol. In this network, each node contends for transmission with an exponentially distributed delay value. We manipulate the mean of the backoff delay to control the transmission aggressiveness of each node and see its impacts on RNC throughput. At $t = 0$ms, the mean backoff delay of each node is set such that all the destination nodes, node $4, 5, 6$, are transmitting at about 0.12pkt/ms. Subsequently, at $t = 1000\text{ms}, t = 2000\text{ms}$ and $t = 3000$ms, the mean backoff delay of nodes $1, 4, 6$ are reduced, i.e., transmission aggressiveness increased, respectively as follows. The mean backoff delay of node 1 is reduced from 3.70ms to 2.24ms, node 4 from 2.74ms to 1.66ms, and node 6 from 1.66ms to 0.83ms. Figure 2.2(b) shows that, for example, at $t = 2000$ms, when node 4 starts to contend more aggressively, it improves the throughput of node 6. However, this simultaneously leads to the drop of the throughput of node 4 itself and node 5. An apparent reason is that it leads to reduced channel availability for these two nodes. Similar effects can also be seen for the subsequent window size change when node 6 becomes more aggressive.

Both of the above two examples, one at the PHY layer, and the other at the MAC layer, show that due to the network dynamics and the complexity of the problem, it would be cumbersome or unsuccessful to employ some static, or heuristic resource allocation mechanism in a network employing RNC. Rather, a deliberately designed, and more importantly, dynamic resource allocation algorithm is required to support the optimal RNC performance. Since RNC is fundamentally different from routing and forwarding in terms of packet delivery as there are no specific routes being computed and followed [14], analyzing it with traditional methods designed for uncoded networks will be problematic, because adopting an inappropriate model will not take full advantage of the benefits that RNC offers, such as the fact that RNC utilizes wireless network's broadcast effect. In light of this, a differential equation based framework in [15] and [16] is of particular interest for deriving resource allocation algorithms for RNC. This framework leverages a system of differential equations to elegantly model the rank evolution process which shapes the RNC performance. The presence of PHY and MAC layer parameters in this model makes it natural to analyze lower layer resource allocation for RNC.

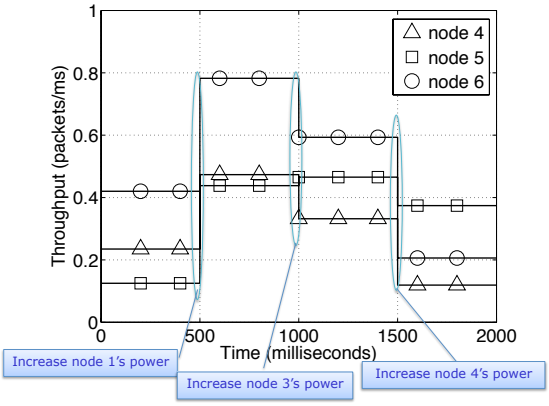

(a) Effect of power on throughput

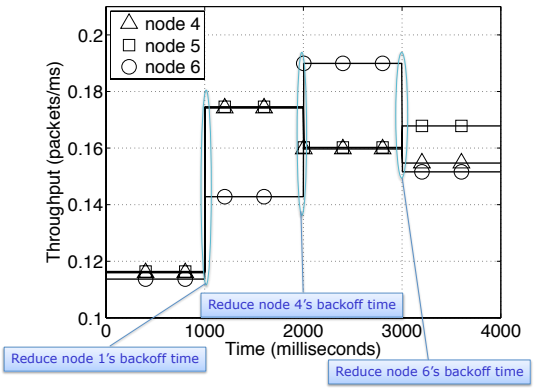

(b) Effect of contention window size on throughput

Figure 2.2: Plot of effect of resource allocation on throughput with the resource being (a) transmit power and (b) CSMA contention window size.

In this chapter, we address the problem of resource allocation for random network coding in wireless networks. In what follows, we first discuss the system model considered in this article and analyze RNC throughput with the differential equation framework in section 2.2. Then in section 2.3, we formulate the resource allocation problem to maximize the minimum network throughput among the destination nodes. While this problem falls into the category of optimal control, which is usually solved by the method of calculus of variations, we present a gradient based framework specifically designed for this resource allocation problem here. This resource allocation framework is guaranteed to reach at a locally maximal solution, and distinguishes itself from all

the other previous works most of which utilize the flow-based formulation of RNC. We will compare our algorithm with the related works after it is introduced in section 2.3. After that, two use cases of this algorithm, i.e., power control and CSMA mean backoff delay control, are presented to improve network coding throughput in section 2.4 and 2.5, respectively. In these two sections, we derive both centralized and online algorithms for the above two use cases. The main contribution of this work is to present a novel methodology to analyze cross-layer resource allocation in the context of RNC from a dynamical system view provided by the differential equation model. The framework utilized in this methodology is sufficiently general such that it can be used to analyze all kinds of PHY/MAC layer resources and derive effective resource allocation algorithms.

2.2 Preliminaries

2.2.1 Differential Equation Framework for RNC

We now present a brief review of the differential equation framework for RNC that is introduced in [15]. A directed hypergraph is adopted in [15] to model a wireless network: $G = (\mathcal{N}, \mathcal{E})$ which has N nodes $\mathcal{N} = \{1, 2, \ldots, N\}$ and hyperarcs $\mathcal{E} = \{(i, \mathcal{K}) | i \in \mathcal{N}, \mathcal{K} \subset \mathcal{N}\}$. The hyperarc $(i, \mathcal{K})$ captures the fact that in a wireless environment, a packet transmitted by node i can be received by a subset of nodes from $\mathcal{K}$. To illustrate this, we note from Figure 2.1 that each node has a point to point link to every other node, but a transmitted packet can only be received by a subset of these nodes. This subset could be determined explicitly by the received signal and interference levels (adopted in section 2.4 for the case of power control), or implicitly by a thresholding distance for reception (adopted in section 2.5 for the case of CSMA).

Consider that each node in the wireless network G is performing random network coding [14], i.e., a source node sends out random linear combinations of the original packets (coded packets), and other nodes merely receive packets from the network and they in turn send out random linear combinations of the packets received. It is assumed that each coded packet is a row vector of length l from $\mathbb{F}_q^l$, where q is the field size. No

routing operations are performed in the network and destination nodes can recover the original packets after collecting sufficient coded packets. Assuming packet loss is only due to bit errors, the probability that a packet transmitted by node i can be received by at least one node in $\mathcal{K}$, $P_{i,\mathcal{K}}$ can be defined as:

$$P_{i,\mathcal{K}} = 1 - \prod_{j \in \mathcal{K}} (1 - P_{i,j}), \tag{2.1}$$

where $P_{i,j}$ is the reception probability of link (i, j). We can see that $P_{i,\mathcal{K}}$ is a function of the PHY layer parameters, e.g., transmit powers and interference. Assuming there exists certain MAC protocol running in its stable state such that node i is sending out coded packets at the average rate of λ_i packets per second, then the successful transmission rate for the hyperarc $(i, \mathcal{K})$ can be defined as:

$$z_{i,\mathcal{K}} = \lambda_i P_{i,\mathcal{K}}. \tag{2.2}$$

$z_{i,\mathcal{K}}$ can also be regarded as the capacity of hyperarc $(i, \mathcal{K})$. Note that the capacity of a cut, $\mathcal{T}$ for $(\mathcal{S}, \mathcal{K})$, $\mathcal{S}, \mathcal{K} \subset \mathcal{N}$ where $\mathcal{K} \subset \mathcal{T} \subset \mathcal{S}^c$ is given as $c(\mathcal{T}) = \sum_{i \in \mathcal{T}^c} z_{i,\mathcal{T}}$. Then, the min cut for $(\mathcal{S}, \mathcal{K})$ is the cut with the minimum size. The number of linearly independent coded packets is called the *rank*, and $V_{\{i\}}$ is used to denote the rank at node i. In essence, $V_{\{i\}}$ is the dimension of the subspace S_i spanned by the coded packets at node i, i.e., $V_{\{i\}} = \dim S_i$. An *innovative* packet of node i is defined as the received packet which increases the rank $V_{\{i\}}$. For a RNC multicast session, if there are m original packets to be delivered, each destination node i can decode only if $V_{\{i\}} = m$. The notion of rank can be naturally extended to a set of nodes, $\mathcal{K}$, and thus $V_{\mathcal{K}}$ is the joint rank of all the nodes from $\mathcal{K}$, i.e., $V_{\mathcal{K}} = \dim S_{\mathcal{K}} = \dim \sum_{i \in \mathcal{K}} S_i$. Note $V_{\mathcal{K}}$ serves as a measure of the amount of information jointly possessed by the set of nodes, $\mathcal{K}$; the decoding process, however, is carried out independently at each destination. We call the stochastic process $V_{\mathcal{K}}(t)$ that grows from 0 to m the rank evolution process.

In [15], it has been shown that under the fluid approximation, a concentration result has been established for the rank evolution process, i.e., the stochastic process $V_{\mathcal{K}}(t)$ is well represented by its mean, $E[V_{\mathcal{K}}(t)]$. Then consider a small time interval Δt in which the number of packets sent from node i that can be successfully received by $\mathcal{K}$

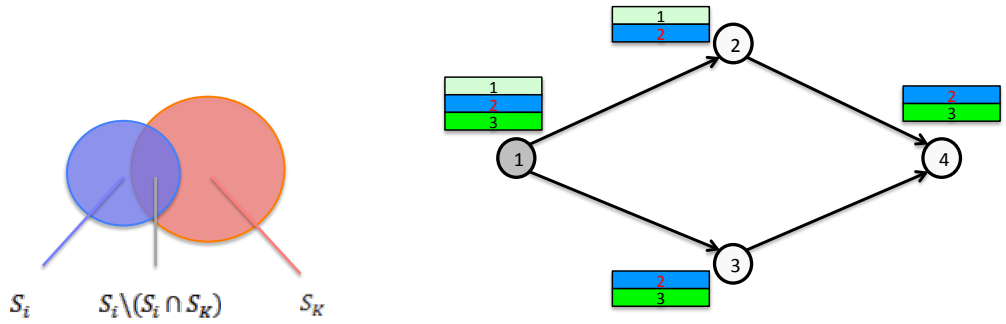

(a) (b)

Figure 2.3: (a) Illustration of the subspace of coded packets that are innovative to $\mathcal{K}$. (b) An illustrative example where node 1 tries to multicast 3 coded packets to node $1, 2$, and 3. The coded packets that each node has are shown next to it. Here, the only packet from node 2 that is innovative to node 4 is packet 1, which is from $S_2 \backslash (S_2 \cap S_4)$.

is $\Delta t z_{i,\mathcal{K}}$. The packets, if received, have to come from the subspace $S_i \backslash (S_i \cap S_{\mathcal{K}})$ to be innovative to the set of nodes, $\mathcal{K}$ (see illustration in Figure 2.3). It can be seen the probability that a coded packet transmitted by node i is actually from $S_i \backslash (S_i \cap S_{\mathcal{K}})$ is given by:

$$\frac{|S_i| - |S_i \cap S_{\mathcal{K}}|}{|S_i|} = \frac{q^{\dim S_i} - q^{\dim S_i \cap S_{\mathcal{K}}}}{q^{\dim S_i}} = \frac{q^{V_i} - q^{V_i + V_{\mathcal{K}} - V_{\{i\} \cup \mathcal{K}}}}{q^{V_i}} = 1 - q^{V_{\mathcal{K}} - V_{\{i\} \cup \mathcal{K}}}. \quad (2.3)$$

Now an equality of the rank increase of $\mathcal{K}$ for the interval Δt can be established:

$$V_{\mathcal{K}}(t + \Delta t) - V_{\mathcal{K}}(t) = \Delta t \sum_{i \notin \mathcal{K}} z_{i,\mathcal{K}} (1 - q^{V_{\mathcal{K}} - V_{\{i\} \cup \mathcal{K}}}) \quad (2.4)$$

Dividing both sides by Δt and then approximating the left hand side with the derivative, we reach at the following system of differential equations:

$$\dot{V}_{\mathcal{K}} = \sum_{i \notin \mathcal{K}} z_{i,\mathcal{K}} (1 - q^{V_{\mathcal{K}} - V_{\{i\} \cup \mathcal{K}}}), \quad \forall \mathcal{K} \subset \mathcal{N} \text{ and } \mathcal{K} \neq \emptyset. \quad (2.5)$$

The derivation of the above differential equations is detailed in [15]. It is worth noting that $\dot{V}_{\mathcal{K}}$ is the rate at which $\mathcal{K}$ is receiving innovative packets, i.e., $\dot{V}_{\mathcal{K}}$ denotes the throughput of $\mathcal{K}$. Apparently, with $z_{i,\mathcal{K}}$ being an abstraction of the outcome of all the PHY/MAC operations in the system of differential equations (2.5), the throughput of

a set of nodes can be elegantly analyzed with respect to PHY/MAC parameters. To illustrate this, we present two numerical examples. First consider a wireless network shown in Figure 2.4(a) (also discussed in [15]) where the source node, node 1 intends to multicast 1000 packets to destination nodes $2, 3, 4$. Let each node perform RNC operations and transmit at 1pkt/ms. Suppose that packets from node 1 can only be successfully received by node 2 and 3, with probability of 0.2 and 0.4, respectively, and node 2 and node 3's packets can only be successfully received by node 4 with probability of 0.6 and 0.7, respectively. Based on the above parameters, we can compute the successful transmission rate $z_{i,\mathcal{K}}$ for each hyperarc $(i, \mathcal{K})$ for this topology. Then all the $z_{i,\mathcal{K}}$ are plugged in the system of differential equations (2.5) and solving them yields the result shown in Figure 2.4(b), the plot of rank evolution process for this RNC multicast. It can be easily verified that the throughputs of the destinations, i.e., the rates at which ranks increase, match the min cuts of every source and destination pair[1]. For instance, it is trivial to see the min cut between node 1 and 2 is 0.2, which is equal to the slope of the straight line for V_2 in Figure 2.4(b). Next, we present an example with a larger topology. Consider the eight-node wireless network shown in Figure 2.5(a). Each line connecting two nodes denotes a bidirectional communication link with the packets reception probability next to the line. This time node 1 has 1000 packets to deliver to node $3, 5$ and 8. We still let each node transmit at 1pkt/ms. The result of solving equations (2.5) for rank evolution is shown in Figure 2.5(b). Again, the system of DEs serve as an accurate analytical model of RNC throughput. The throughputs implied by Figure 2.5(b), i.e., throughputs of nodes $3, 5$ and 8 being 0.4pkt/ms, 0.2pkt/ms, and 0.4pkt/ms, respectively, match the values of min cuts highlighted by the dashed curves in Figure 2.5(a). Thus the DE framework in [15] is versatile and can be used to study the dynamics of RNC in any arbitrary network. In this chapter, we will develop a dynamic radio resource management methodology using this framework.

[1]It is stated in Theorem 1 in [15] that the destination node's throughput computed by equation (2.5) equals the min cut between the source and that destination.

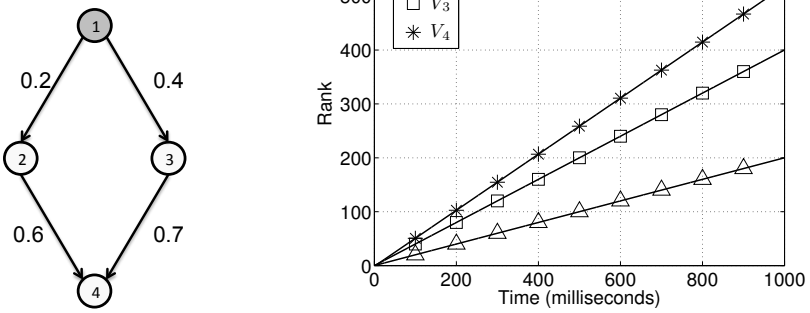

(a) 4-node network topology

(b) Rank evolution

Figure 2.4: Rank evolution modeled by DE, example 1.

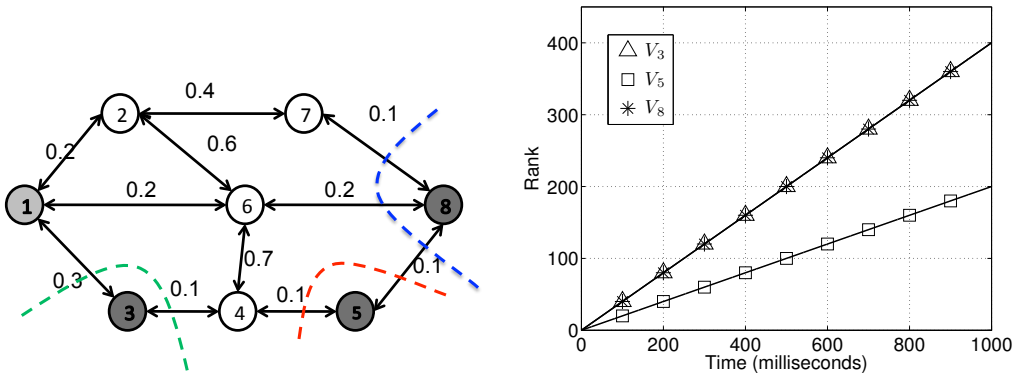

(a) 8-node network topology

(b) Rank evolution

Figure 2.5: Rank evolution modeled by DE, example 2.

2.3 Resource Allocation Algorithm for Wireless Network Coding

2.3.1 Problem Formulation

Consider a wireless network $G = (\mathcal{N}, \mathcal{E})$ which is performing random network coding. The source node s tries to multicast m packets to a set of sink nodes. We proceed to consider some PHY or MAC layer resource at every node i and denote it as r_i. Note that r_i can be any PHY/MAC layer parameter which contributes to the transmission rate λ_i or the packet reception probability $P_{i,\mathcal{K}}$. Letting the vector $\mathbf{r}$ denote $[r_1, r_2, ..., r_N]^\top$,

we have

$$z_{i,\mathcal{K}} = z_{i,\mathcal{K}}(\mathbf{r}), \tag{2.6}$$

i.e., the reception rate $z_{i,\mathcal{K}}$ for each hyperarc $(i, \mathcal{K})$ is an explicit function of allocated resource $\mathbf{r}$. To formulate the resource allocation as an optimization problem for improving the RNC performance, we consider maximizing the minimum throughput among all the sink nodes as the objective function. We let $\mathcal{R}$ be the set of destination nodes which have not reached full rank, m. With a little abuse of notation, we let $\dot{V}_i$ denote $\dot{V}_{\{i\}}$. Then letting $k = \arg\min_{j\in\mathcal{R}} \dot{V}_j$, we construct the following optimization problem:

$$\begin{aligned}
\text{maximize} \quad & \dot{V}_k \\
\text{subject to} \quad & \dot{V}_{\mathcal{K}} = \sum_{i\notin\mathcal{K}} z_{i,\mathcal{K}} \cdot (1 - q^{V_{\mathcal{K}} - V_{\{i\}\cup\mathcal{K}}}),\ \forall \mathcal{K} \subset \mathcal{N}. \\
& z_{i,\mathcal{K}} = z_{i,\mathcal{K}}(\mathbf{r}). \\
& k = \arg\min_{j\in\mathcal{R}} \dot{V}_j \\
\text{variables} \quad & \mathbf{r}.
\end{aligned} \tag{2.7}$$

2.3.2 Gradient-based Resource Allocation Algorithm

Note that in general, the optimization problem given by (2.7) is not convex, and thus it is difficult to find the globally optimal solution. Additionally, this type of problem which is constrained by a set of first-order differential equations can be categorized into an optimal control problem. Existing approaches to optimal control involve calculus of variations, which can be computationally expensive and intractable in wireless networks. In this chapter, we aim to find a local optimum of this problem which can provide significant throughput gains with less computational complexity. We take an approach based on the steepest ascent (its counterpart for minimization problems is called steepest descent, see [17]), i.e. adjust the resource $\mathbf{r}$ towards the direction of the gradient. Essentially, our optimization objective, $\dot{V}_k$ is a function of the resource $\mathbf{r}$, i.e., $\dot{V}_k = \dot{V}_k(\mathbf{r})$. This allows us to establish the gradient of throughput as the direction of the dynamic adjustment of the resource, i.e.,

$$\dot{\mathbf{r}} = a' \cdot \nabla \dot{V}_k, \tag{2.8}$$

where a' is a positive constant tuning the gain. In this way, the allocation of resource will be iterative, as well as dynamic. We consider a discrete approximation to compute the derivative in equation (2.8) as follows. Let Δv be the step size, and $\mathbf{e}_i$ be a column vector with 1 being the ith component and 0 elsewhere. Writing in component-wise form, we have

$$\dot{r}_i = a' \cdot \frac{\dot{V}_k(\mathbf{r} + \Delta v \mathbf{e}_i) - \dot{V}_k(\mathbf{r})}{\Delta v}. \tag{2.9}$$

Replacing $a'/\Delta v$ with a, we have:

$$\dot{r}_i = a \cdot \left(\dot{V}_k(\mathbf{r} + \Delta v \mathbf{e}_i) - \dot{V}_k(\mathbf{r}) \right). \tag{2.10}$$

Equation (2.10) serves as the basis of the resource allocation algorithm and works in an iterative manner to adapt the resource allocation towards the direction of the approximated gradient of the minimum throughput. Our algorithm stops when, at certain iteration, $\dot{\mathbf{r}} \leq \boldsymbol{\epsilon}$ is achieved for a sufficiently small vector $\boldsymbol{\epsilon}$. In the above, $\dot{V}_k$ is given by equation (2.5) and thus the allocation of resources takes into consideration the latest network throughput information and therefore also works in a dynamic fashion. It has been proved in [13] that the algorithm given by equation (2.10) converges to a local maximum. [13] also pointed out that the gain parameter a should be chosen such that $q^{1/a} \ll 1$ and $q^a \gg 1$.

Note that until now, we have not imposed any specific models for the PHY/MAC layers. In fact, the resource allocation approach presented here is flexible enough that it can work with any specific lower layer models/mechanisms. For a better elucidation of this approach, we illustrate its applicability by solving two practical allocation problems for RNC in following sections: (i) power control for maximizing the minimum throughput, and (ii) CSMA mean backoff delay control for maximizing the minimum throughput. Before that, we first discuss the the differences between our framework and the previous resource allocation frameworks for RNC.

2.3.3 Relationship to existing literature on resource allocation for RNC

The topic of resource allocation for RNC was first visited by Lun *et al.* in [9] where the authors considered associating a cost function for each hyperarc and minimizing the total cost for the whole network. Since [9], a number of works focused on more specific problems of crosslayer optimization, such as power control and scheduling [10] [11] for RNC. When lower layers' parameters are considered, the crosslayer resource optimization problems tend to be non-convex. Like the other works, our resource allocation framework is able to yield locally optimal allocation for such non-convex problems, as proved in [13]. Apart from this, our resource allocation algorithm distinguishes itself from most of the previous works of the similar topic owing to the use of the differential equation model of RNC, which not only augments the algorithmic design space for RNC resource allocation, but brings many merits over the other algorithms based upon the network flow model, e.g. the one used in [9]. First of all, our framework is dynamic. Note the common methodology of most flow based algorithms [10] [11] is to establish a network utility function as the optimization objective and consider wireless hyperarc capacities, formulated with network flows, as constraints. One invariable feature of these works is that the utility function and hyperarc capacities considered are not time-dependent but static. Therefore, for instance, in [11] which considers fading, fading has to be studied through its ergodic behavior. Due to the lack of time-dependency when setting up the optimization framework for resource allocation for RNC, if any of the underlying dynamic network elements, such as channel, network connection, or MAC/PHY configuration, alter, the utility maximization based optimization framework needs to be updated. On the other hand, since our differential equation based resource allocation framework is built upon the theory of dynamical systems, it is inherently capable of accommodating the dynamism of the network: the underlying parameters λ_i and $P_{i,j}$, which capture MAC and PHY characteristics respectively, are in fact modeled to be time dependent. They evolve together with the rank V_j naturally. Thus our framework provides an accurate model for such dynamic interaction between network

resources and RNC performance whereas the other existing models do not. Second, our framework is less complex. Note with flow based model, it is known how to solve for the RNC throughput $\dot{V}_j$. However, that is done by i) setting up a network flow based formulation where flow sizes are bounded by hyperarc capacities, which in turn are determined by the lower layer resources, and ii) solving this formulated problem for the min cut between the source and the destination node. In other words, it can be seen that flow-based models as adopted in [10] [11] do not explicitly model $\dot{V}_j$, and thus the resources to be allocated have to be placed in the constraints when being optimized. The differential equation model of RNC, on the other hand, explicitly describes $\dot{V}_j$ in terms of PHY and MAC parameters, λ_i and $P_{i,j}$. This allows resource allocation for RNC to be directly the objective of the optimization problem formulated, rather than constraints, e.g., in equation (2.7) $\dot{V}_k$ is actually given by $\dot{V}_k = \sum_{i \neq k} \lambda_i P_{i,k} \cdot (1 - q^{V_k - V_{\{i,k\}}})$. Thus it substantially simplifies algorithm design for such resource allocation. Specifically, this allows us to apply a very fundamental line search algorithm based on the idea of gradient ascent for unconstrained optimization, and effectively solve the RNC resource allocation, as will be illustrated later.

2.4 Dynamic Power Control in RNC

There exists a rich history of transmit power control for cellular networks (see [18]) where the goal was to minimize the total power levels [19–21], or to maximize network utilities [22–24]. In this section, however, we consider performing power control in a coded wireless network to improve RNC throughput and design a centralized power control algorithm, as well as an online version of it which is more amenable to implementation.

2.4.1 Interference Model

While the gradient based resource allocation framework in section 2.3 is applicable for any wireless network with RNC, in this section we will specifically illustrate its use for power control in a network where we model the interference as Gaussian. Here we also

assume the wireless network G to be interference limited, and model each point-to-point link gain h_{ji} for (i,j) with a path loss model. We use P_i^{Tx} to denote the transmit power at node i. The received signal level is given by $P_i^{\mathrm{Tx}} h_{ji}$. Each node i is assumed to implement a certain processing gain g_i. Therefore, when node j intends to receive the signal transmitted by i, the aggregated interference power is

$$J_{ji} = \sum_{m \neq j,i} (P_m^{\mathrm{Tx}} \cdot h_{jm}/g_i). \tag{2.11}$$

Let σ^2 denote the noise power. The signal-to-noise-and-interference ratio (SINR) for the point-to-point link (i,j) can be written as

$$SINR_{(i,j)} = \frac{P_i^{\mathrm{Tx}} \cdot h_{ji}}{J_{ji} + \sigma^2}. \tag{2.12}$$

Assuming BPSK signaling and Gaussian interference, the bit error rate for sender-receiver pair (i,j) is given as

$$p_{i,j}^{\mathrm{bit}} = Q\left(\sqrt{SINR_{(i,j)}}\right). \tag{2.13}$$

Further, assuming each packet is of l bits, the probability that node j can receive a packet without error is

$$P_{i,j} = (1 - p_{i,j}^{\mathrm{bit}})^l. \tag{2.14}$$

Note that the differential equation framework requires the computation of $P_{i,\mathcal{K}}$ given in equation (2.1). Under the above interference model, we assume that there is a MAC protocol running in steady state such that each node i has an average transmission rate λ_i. Therefore, $z_{i,\mathcal{K}}$ in equation (2.2) can be now written as:

$$\begin{aligned} z_{i,\mathcal{K}} &= \lambda_i P_{i,\mathcal{K}} \\ &= \lambda_i \cdot \left(1 - \prod_{j \in \mathcal{K}} \left(1 - \left(1 - Q\left(\sqrt{\frac{P_i^{\mathrm{Tx}} \cdot h_{ji}}{\sum_{m \neq j,i} (P_m^{\mathrm{Tx}} \cdot h_{jm}/g_i) + \sigma^2}}\right)\right)^l\right)\right). \end{aligned} \tag{2.15}$$

2.4.2 Centralized Power Control

Let $\mathbf{P}^{\mathrm{Tx}} = \left[P_1^{\mathrm{Tx}}, P_2^{\mathrm{Tx}}, ..., P_N^{\mathrm{Tx}}\right]^\top$ be the transmit power vector and the resource $r_i = P_i^{\mathrm{Tx}}$. The centralized power control algorithm follows directly from equation (2.10) (see also [25] and [13]):

$$\dot{P}_i^{\mathrm{Tx}} = a \cdot \left(\dot{V}_k(\mathbf{P}^{\mathrm{Tx}} + \Delta v \mathbf{e}_i) - \dot{V}_k(\mathbf{P}^{\mathrm{Tx}}) \right), \tag{2.16}$$

where

$$\dot{V}_k = \sum_{i \neq k} \lambda_i \cdot \left(1 - Q\left(\sqrt{\frac{P_i^{\mathrm{Tx}} \cdot h_{ki}}{\sum_{m \neq k,i} (P_m^{\mathrm{Tx}} \cdot h_{km}/g_i) + \sigma^2}} \right) \right)^l \cdot \left(1 - q^{V_k - V_{\{i,k\}}}\right), \tag{2.17}$$

based on the interference model above. Further, we consider dividing the time into equal length intervals, and only computing and applying power update at the end of each interval. Then we can rewrite the above algorithm in a discretized and iterative form:

$$\mathbf{P}^{\mathrm{Tx},n} = \mathbf{P}^{\mathrm{Tx},n-1} + a \cdot \mathbf{B}(\mathbf{P}^{\mathrm{Tx},n-1}), \quad n = 2, 3, 4, ... \tag{2.18}$$

where we use a superscript n to denote a parameter evaluated at nth iteration, e.g. $\mathbf{P}^{\mathrm{Tx},n}$ is $\mathbf{P}^{\mathrm{Tx}}$ at the nth iteration, and $\mathbf{B}(\mathbf{P}^{\mathrm{Tx}})$ is a vector defined such that its ith component is given by:

$$B_i(\mathbf{P}^{\mathrm{Tx}}) = \dot{V}_k(\mathbf{P}^{\mathrm{Tx}} + \Delta v \mathbf{e}_i) - \dot{V}_k(\mathbf{P}^{\mathrm{Tx}}). \tag{2.19}$$

In fact, $\mathbf{B}$ is the direction to which we update $\mathbf{P}^{\mathrm{Tx}}$ such that $\dot{V}_k$ is improved; thus $\mathbf{B}$ is a gradient ascent direction.

We assume there is a certain power budget at each node i, i.e., $0 \leq P_i^{\mathrm{Tx}} \leq P_i^{\max}$. Considering this, the algorithm can be summarized as:

$$\begin{aligned}
&k = \arg\min_{j \in \mathcal{R}} \dot{V}_j^{n-1} \\
&B_i(\mathbf{P}^{\mathrm{Tx},n-1}) = \dot{V}_k(\mathbf{P}^{\mathrm{Tx},n-1} + \Delta v \mathbf{e}_i) - \dot{V}_k(\mathbf{P}^{\mathrm{Tx},n-1}) \\
&P_i^{\mathrm{Tx},n} = \begin{cases}
P_i^{\mathrm{Tx},n-1}, & \text{if } P_i^{\mathrm{Tx},n-1} + a \cdot B_i(\mathbf{P}^{\mathrm{Tx},n-1}) > P_i^{\max} \text{ and} \\
& B_i(\mathbf{P}^{\mathrm{Tx},n-1}) > 0, \\
& \text{or } P_i^{\mathrm{Tx},n-1} + a \cdot B_i(\mathbf{P}^{\mathrm{Tx},n-1}) < 0 \text{ and} \\
& B_i(\mathbf{P}^{\mathrm{Tx},n-1}) < 0; \\
P_i^{\mathrm{Tx},n-1} + a \cdot B_i(\mathbf{P}^{\mathrm{Tx},n-1}), & \text{otherwise.}
\end{cases}
\end{aligned} \tag{2.20}$$

It is assumed that there exists a central controller which knows the exact analytical expression of $\dot{V}_k(\mathbf{P}^{\mathrm{Tx}})$, so that based on equation (2.19), $B_i(\mathbf{P}^{\mathrm{Tx}})$ can be evaluated to obtain the ascent direction. We thus call it a *centralized* resource allocation algorithm.

2.4.3 Online Power Control

Motivation for online power control algorithm

While the algorithm in section 2.4.2 is effective in achieving the objective to improve network coding throughput [13], it can be further improved for the purpose of implementation. Specifically, the centralized algorithm, specified in equation (2.20), works by adjusting powers towards an ascent direction, $\mathbf{B}(\mathbf{P}^{\mathrm{Tx}})$, which is an approximation of the gradient $\nabla_{\mathbf{P}^{\mathrm{Tx}}}\dot{V}_k$, i.e., $\mathbf{B}(\mathbf{P}^{\mathrm{Tx}}) \approx \nabla_{\mathbf{P}^{\mathrm{Tx}}}\dot{V}_k$. Therefore in the centralized algorithm, $B_i(\mathbf{P}^{\mathrm{Tx}})$ has to be evaluated. From equation (2.19) we can see that this in turn requires the exact analytical formula for $\dot{V}_k(\mathbf{P}^{\mathrm{Tx}})$ be known. If one were to implement it in a wireless network, obtaining or in some manner accurately estimating such exact formulas might be an intimidating, or even infeasible task. To circumvent this problem, we seek another algorithm which produces a better estimation of $\nabla_{\mathbf{P}^{\mathrm{Tx}}}\dot{V}_k$, denoted by $\mathbf{B}'(\mathbf{P}^{\mathrm{Tx}})$, in a sense that it has the following desirable properties: i) it would perform similarly well as the centralized algorithm to improve RNC performance, however with only a minimal amount of knowledge about the network; ii) this knowledge could be learnt by every node through a limited amount of message passing such that the algorithm can operate online, i.e., each node exchanges control messages with the network, computes the power update for itself based on the information obtained and adjusts its power without any noticeable delay. In the following, we first describe a method to estimate $\mathbf{B}'(\mathbf{P}^{\mathrm{Tx}})$ with reduced network state knowledge, and then discuss possible aspects to take into consideration when implementing this algorithm.

Deriving the online algorithm

We seek a better estimation of the gradient $\nabla^n_{\mathbf{P}^{\mathrm{Tx}}}\dot{V}_k$, written as $\mathbf{B}'(\mathbf{P}^{\mathrm{Tx},n})$, at the end of interval n based on the network information available. The goal is to use $\mathbf{B}'(\mathbf{P}^{\mathrm{Tx}})$ when computing the power updates:

$$\mathbf{P}^{\mathrm{Tx},n} = \mathbf{P}^{\mathrm{Tx},n-1} + a \cdot \mathbf{B}'(\mathbf{P}^{\mathrm{Tx},n-1}), \quad n = 2, 3, 4, ... \tag{2.21}$$

Before starting deriving the online algorithm, we first introduce the following notations:

- Let $\dot{\mathbf{V}}$ denote the size-(2^N-1) throughput vector, consisting of $\dot{V}_{\mathcal{K}}, \forall \mathcal{K} \subset \mathcal{N}, \mathcal{K} \neq \emptyset$. More precisely, $\dot{\mathbf{V}}$ is given by

$$\dot{\mathbf{V}} = \left[\dot{V}_{\{1\}}\ \dot{V}_{\{2\}}\ \dot{V}_{\{1,2\}}\ \dot{V}_{\{3\}}\ ...\ \dot{V}_{\{1,2,...,N\}}\right] \tag{2.22}$$

- Let $\mathbf{z}$ denote the size-$\big(N \cdot (2^N-1)\big)$ packet reception rate vector, consisting of $z_{i,\mathcal{K}}, \forall i \in \mathcal{N}, \mathcal{K} \subset N, \mathcal{K} \neq \emptyset$. For each i, $z_{i,\mathcal{K}}, \forall \mathcal{K} \subset \mathcal{N}$ is arranged similarly with $\dot{\mathbf{V}}$. Then $\mathbf{z}$ is given by concatenating $z_{i,\mathcal{K}}, \forall \mathcal{K} \subset \mathcal{N}, \mathcal{K} \neq \emptyset$ from $i=1$ to $i=N$:

$$\mathbf{z} = \left[z_{1,\{1\}}\ z_{1,\{2\}}\ z_{1,\{1,2\}}\ ...\ z_{1,\{1,2,...,N\}}\ ...\ z_{N,\{1,2,...,N\}}\right] \tag{2.23}$$

- Let $z'_{i,\mathcal{K}}$ denote the innovative packet reception rate of hyperarc $(i,\mathcal{K})$.

- Let $\mathbf{z}'$ denote the size-$\big(N \cdot (2^N-1)\big)$ innovative packet reception rate vector, consisting of $z'_{i,\mathcal{K}}, \forall (i,\mathcal{K}) \in \mathcal{E}$. By replacing every $z_{i,\mathcal{K}}$ of $\mathbf{z}$ with $z'_{i,\mathcal{K}}$, we get $\mathbf{z}'$.

Unlike the way the centralized algorithm works to directly approximate $\nabla_{\mathbf{P}^{\mathrm{Tx}}}\dot{V}_k$, here $\dot{V}_k$ is viewed as a composition of $\mathbf{z}$ which is again a composition of $\mathbf{P}^{\mathrm{Tx}}$. More precisely, since we have $\dot{V}_k = \dot{V}_k(\mathbf{z})$ and $\mathbf{z} = \mathbf{z}(\mathbf{P}^{\mathrm{Tx}})$, then based on the chain rule, $\nabla_{\mathbf{P}^{\mathrm{Tx}}}\dot{V}_k$ can be derived as:

$$\nabla_{\mathbf{P}^{\mathrm{Tx}}}\dot{V}_k = \nabla_{\mathbf{z}}\dot{V}_k J_{\mathbf{P}^{\mathrm{Tx}}}\mathbf{z}, \tag{2.24}$$

where $\nabla_{\mathbf{z}}\dot{V}_k$ and $J_{\mathbf{P}_{\mathrm{T}}}\mathbf{z}$ are the gradient of $\dot{V}_k$ with respect to $\mathbf{z}$ and the Jacobian of $\mathbf{z}$ with respect to $\mathbf{P}^{\mathrm{Tx}}$, respectively. Note that from the above equation on, we temporarily drop the superscript n to simplify the notation. Equation (2.24) provides the exact formula for computing the gradient of $\dot{V}_k$. To derive the online algorithm, we shall investigate both terms on the right hand side one after another.

Referring to equation (2.23), and noting $\dot{V}_k = \sum_{i \notin k} z_{i,k} \cdot (1 - q^{V_k - V_{\{i,k\}}})$, we have

$$\nabla_{\mathbf{z}}\dot{V}_k = \left[0, 1-q^{V_k-V_{\{1,k\}}}, 1-q^{V_k-V_{\{2,k\}}}, 0, ..., 0, 1-q^{V_k-V_{\{k-1,k\}}}, 0, ..., 0, 1-q^{V_k-V_{\{k+1,k\}}}, ...\right]. \tag{2.25}$$

Noting $\nabla_{\mathbf{z}}\dot{V}_k$ has $(N-1)$ non-zero components: $1-q^{V_k-V_{\{i,k\}}}, \forall i \in \mathcal{N}, i \neq k$, we would like to avoid evaluating $\nabla_{\mathbf{z}}\dot{V}_k$ since it requires the knowledge of $V_{\{i,k\}}$, the joint rank of node i and k. Obtaining such joint rank in a wireless network would be cumbersome

because it requires plenty of information to be exchanged. Instead, note that $z_{i,\mathcal{K}}$ is defined as the packet reception rate, and $(1-q^{V_{\mathcal{K}}-V_{\{i\}\cup\mathcal{K}}})$ is the probability that the received packet is an innovative packet. Then the innovative packet reception rate $z'_{i,\mathcal{K}}$ is given by $z'_{i,\mathcal{K}} = z_{i,\mathcal{K}} \cdot (1-q^{V_{\mathcal{K}}-V_{\{i\}\cup\mathcal{K}}})$. Therefore, we take an alternative approach to consider obtaining the gradient with respect to the innovative packet reception rate $\mathbf{z}'$ instead of $\mathbf{z}$, i.e., $\nabla_{\mathbf{z}'}\dot{V}_k$. With $\mathbf{z}'$, we can rewrite equation (2.5) in a more compact form:

$$\dot{V}_{\mathcal{K}} = \sum_{i\notin\mathcal{K}} z'_{i,\mathcal{K}},\ \forall\mathcal{K}\subset\mathcal{N}, \tag{2.26}$$

and $\nabla_{\mathbf{z}'}\dot{V}_k$ can be derived accordingly as:

$$\nabla_{\mathbf{z}'}\dot{V}_k = [0,\ 1,\ 1,\ 0,\ ...,\ 0,\ 1,\ 0,\ ...,\ 0,\ 1,\ 0,\ ...\ 0]\,. \tag{2.27}$$

Then the gradient of $\dot{V}_k$ can be calculated by

$$\nabla_{\mathbf{P}^{\mathrm{Tx}}}\dot{V}_k = \nabla_{\mathbf{z}'}\dot{V}_k J_{\mathbf{P}^{\mathrm{Tx}}}\mathbf{z}'. \tag{2.28}$$

Thus the evaluation of $\nabla_{\mathbf{P}^{\mathrm{Tx}}}\dot{V}_k$ in equation (2.28) boils down to the evaluation of $J_{\mathbf{P}^{\mathrm{Tx}}}\mathbf{z}'$. Note we would avoid the approach of directly evaluating it as this would again require that the underlying PHY layer specifics of all the nodes be known universally, such that the analytical formula of $\mathbf{z}'$ is known. Furthermore, computing the Jacobian, i.e., $J_{\mathbf{P}^{\mathrm{Tx}}}\mathbf{z}'$ can be computationally prohibitive. Rather, we numerically estimate this Jacobian at each iteration by following a similar approach that is adopted in Broyden's method [26]. For that purpose, we recover the superscript n to denote the parameters evaluated at the nth interval. Each interval is of equal-length (corresponding to the time between successive power updates) and is assumed to be of τ seconds. Then according to [26], we have

$$\hat{J}^n_{\mathbf{P}^{\mathrm{Tx}}}\mathbf{z}' = \hat{J}^{n-1}_{\mathbf{P}^{\mathrm{Tx}}}\mathbf{z}' + \frac{\Delta\mathbf{z}'^n - \hat{J}^{n-1}_{\mathbf{P}^{\mathrm{Tx}}}\mathbf{z}'\Delta\mathbf{P}^{\mathrm{Tx},n}}{\|\Delta\mathbf{P}^{\mathrm{Tx},n}\|^2}\Delta\mathbf{P}^{\mathrm{Tx},n\top}, \tag{2.29}$$

where $\Delta\mathbf{z}'^n = \mathbf{z}'^n - \mathbf{z}'^{n-1}$, $\Delta\mathbf{P}^{\mathrm{Tx},n} = \mathbf{P}^{\mathrm{Tx},n} - \mathbf{P}^{\mathrm{Tx},n-1}$, and $\hat{J}^n_{\mathbf{P}^{\mathrm{Tx}}}\mathbf{z}'$ is the estimation of the Jacobian in the nth interval.

We can estimate the average innovative packets reception rate in each time interval which is of length τ, i.e.,

$$z'^n_{i,j} = c^n_{i,j}/\tau, \tag{2.30}$$

where $c_{i,j}^n$ is the number of innovative packets sent by node i that node j has received in the nth time interval. Note that the granularity of power updates are based on this time interval. Now we can summarize below the expression for the estimation of $\nabla_{\mathbf{P}^{\mathrm{Tx}}}^n \dot{V}_k$, $\mathbf{B}'(\mathbf{P}^{\mathrm{Tx},n})$, given by the online algorithm:

$$\mathbf{B}'(\mathbf{P}^{\mathrm{Tx},n}) = \nabla_{\mathbf{z}'}^n \dot{V}_k \hat{J}_{\mathbf{P}^{\mathrm{Tx}}}^n \mathbf{z}'. \tag{2.31}$$

Finally, the transmit powers are adapted according to the following equation

$$\mathbf{P}^{\mathrm{Tx},n} = \mathbf{P}^{\mathrm{Tx},n-1} + a \cdot \mathbf{B}'(\mathbf{P}^{\mathrm{Tx},n-1}), \quad n = 2, 3, 4, ... \tag{2.32}$$

where a is the gain parameter for power control.

Discussion regarding implementation considerations.

This algorithm can be naturally implemented in a distributed way with the help of a message exchange protocol. This protocol will be implemented to broadcast only one type of message which includes three pieces of information: innovative packets counts, its current rank and power, i.e., in each interval, node j sends a message containing $z'_{i,j}$ for every i, V_j and P_j^{Tx}. Each node is running an instance of the online algorithm and computes the gradients for every node in the network, but will only update its own power based on its own computation.

Note to initiate the algorithm, we need to provide an initial estimate of $J_{\mathbf{P}^{\mathrm{Tx}}}\mathbf{z}'$, i.e., $J^0_{\mathbf{P}^{\mathrm{Tx}}}\mathbf{z}'$ and randomly generate the first power update. To detect the convergence of the online algorithm, a threshold value, which can be an achievable and satisfactory throughput value, should be set. In any interval i, the numerical value of $\dot{V}_k^i$ is monitored and if it grows larger than the threshold, the algorithm will maintain the previous allocation; otherwise, the gradient will be estimated and power at each node will be adjusted. Moreover, to refrain from unduly large gradient update which might lead the algorithm to an unstable state, we observe the results given by (2.31) and if the gradient is larger than a threshold $\mathbf{s}$, we normalize the gradient, i.e.,

$$\mathbf{B}'(\mathbf{P}^{\mathrm{Tx},n}) = \begin{cases} \frac{\nabla_{\mathbf{z}'}^n \dot{V}_k \hat{J}_{\mathbf{P}^{\mathrm{Tx}}}^n \mathbf{z}'}{\|\nabla_{\mathbf{z}'}^n \dot{V}_k \hat{J}_{\mathbf{P}^{\mathrm{Tx}}}^n \mathbf{z}'\|}, & \text{if } \nabla_{\mathbf{z}'}^n \dot{V}_k \hat{J}_{\mathbf{P}^{\mathrm{Tx}}}^n \mathbf{z}' \geq \mathbf{s} \\ \nabla_{\mathbf{z}'}^n \dot{V}_k \hat{J}_{\mathbf{P}^{\mathrm{Tx}}}^n \mathbf{z}', & \text{otherwise.} \end{cases} \tag{2.33}$$

We summarize this algorithm in Algorithm 1.

Algorithm 1 Online network coding aware power control algorithm

$\tau \leftarrow$ Power update granularity

$\tau_0 \leftarrow$ Time interval to make gradient computation

rand(N,1) $\leftarrow$ length-N random vector with each element larger than -0.5 and less than 0.5

$\mathbf{c}^0 \leftarrow \mathbf{0}$: counters for number of innovative packets.

$\mathbf{P}^{\mathrm{Tx},0} \leftarrow \mathbf{P}^{\mathrm{init}}$

$J^0_{\mathbf{P}^{\mathrm{Tx}}}\mathbf{z}' \leftarrow J_{\mathbf{P}^{\mathrm{Tx}}}\mathbf{z}'^{\mathrm{init}}$

while $t \leq \tau$ **do**

update $\mathbf{c}^0$

end while

compute $\mathbf{z}'^0$

$\mathbf{P}^{\mathrm{Tx},1} = \mathbf{P}^{\mathrm{Tx},0} + \mathrm{rand}(N,1)$

$n \leftarrow 1$

while $n\tau \leq t \leq (n+1)\tau$ **do**

update $\mathbf{c}^n$

if $t > (n+1)\tau - \tau_0$ **then**

while $\mathbf{B}'(\mathbf{P}^{\mathrm{Tx},n})$ has not been computed **do**

compute $\mathbf{z}'^n$

$\Delta\mathbf{P}^{\mathrm{Tx},n} = \mathbf{P}^{\mathrm{Tx},n} - \mathbf{P}^{\mathrm{Tx},n-1}$

$\Delta\mathbf{z}'^n = \mathbf{z}'^n - \mathbf{z}'^{n-1}$

Compute $\hat{J}^n_{\mathbf{P}^{\mathrm{Tx}}}\mathbf{z}'$ as in (2.29)

Compute $\mathbf{B}'(\mathbf{P}^{\mathrm{Tx},n})$ as in (2.31)

Set power $\mathbf{P}^{\mathrm{Tx},n} = \mathbf{P}^{\mathrm{Tx},n-1} + a \cdot \mathbf{B}'(\mathbf{P}^{\mathrm{Tx},n-1})$

$n \leftarrow n+1$

end while

end if

end while

2.4.4 Numerical Results

We use two ways to evaluate the power control algorithm for random network coding. First, for the centralized algorithm, we use a numerical differential equation solver to simultaneously solve the differential equations in equation (2.5) and (2.20). According to the results of evaluating the gradient ascent direction $\mathbf{B}(\mathbf{P}^{\mathrm{Tx},n-1})$ given in (2.20), the power levels are updated at the end of each iteration n in the differential equation solver. Second, for the online algorithm, we implement the algorithm with an event-driven simulation in MATLAB.

For the evaluations, we consider the topology of a 6-node network as shown in Figure 2.1. This network is assumed to be running random network coding, i.e., original packets are being coded at each node, and the intended destination nodes decode to recover them. Therefore, the original packets are not "routed" towards the destination nodes. The goal is for a sender node, node 1, to multicast 2000 packets to a set of sink nodes, node $4, 5, 6$. We assume there is a path loss model for each point to point link in this network. We use the ITU model for indoor propagation [27], where the path loss of the transmission from node i to node j, PL_{ji} is given by:

$$\mathrm{PL}_{ji} = 20 \log f + 10n \log d_{ji} + P_f(n) - 28. \tag{2.34}$$

In this evaluation, the transmitted signal frequency f is set to be 2.4GHz, path loss exponent n to be 3, and floor penetration factor $P_f(n)$ to be 11. Thus the link gain for (i, j) can be computed as $h_{ji} = 10^{\mathrm{PL}_{ji}/10}$.

Centralized algorithm

Figure 2.6 shows the results of throughput and power adjustment of the centralized power control algorithm. In Figure 2.6(a), we can see that without power control, the throughputs of the three destination nodes, node $4, 5, 6$ are all less than 0.5pkt/ms, and the minimum of them is less than 0.25pkt/ms. With dynamic power control, the throughput of all the nodes is improved. From around $t = 400$ms, the throughputs begin to converge to the same value, 1pkt/ms. Since each node, including the source node, has a transmission rate of 1pkt/ms, the optimal multicast throughput is also

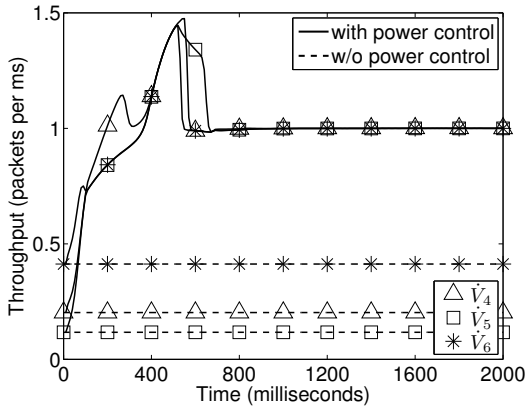

(a) Effect of power control on throughput

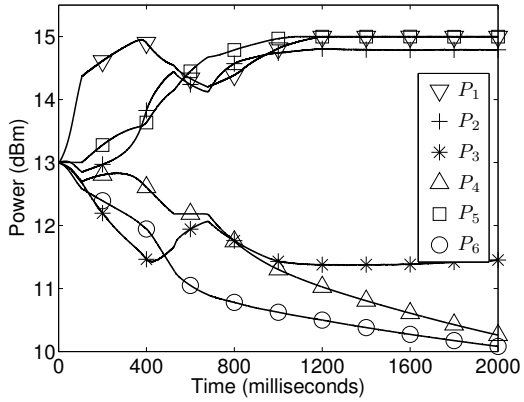

(b) Power adjustment

Figure 2.6: Centralized power control (a) Throughput, (b) power adjustment.

1pkt/ms and the centralized algorithm achieves this optimum, thereby showing that this network coding aware power control regains the broadcast advantage. From Figure 2.6(b) we can see that the transmit power at each node is continuously adjusted by the power control algorithm. When the algorithm is started, i.e., $t = 0$ms, powers of node $1, 2, 5$ are increased, on the other hand, other nodes' power are suppressed. When approaching throughput convergence, the algorithm sets the powers of nodes $1, 2, 5$ to about 15dBm, and all the other nodes' powers to less than 12dBm.

Comparison between DE-based centralized algorithm and flow-based algorithm

We also compare the formulation and performance of the dynamic power control algorithm with those of a benchmark algorithm that uses a flow-based model. In the benchmark algorithm, the max-min throughput problem is formulated similarly with [9]; in the meantime, it also accommodates PHY layer configurations. Specifically, for each destination $d \in \mathcal{R}$, there is a flow f^d associated with it. To make the interference tractable with the network flow model, we consider that this network uses TDMA for media access control and assume unicast communication. We further assume that each node i uses the same power for transmissions on all its outgoing links. Let $t_{i,j}$ denote the time fraction that node i allocates to link (i,j) and E denote the set of all the point-to-point links.

Let W_i be the throughput of node i, N_i be the neighbor nodes of node i which can transmit to or receive from node i. $\lambda_i = 1$pkt/ms is the rate that node i is transmitting. Then an equivalent formulation of the max-min throughput problem described in equation (2.7) with respect to power control is given for the network flow model as follows:

$$\text{maximize} \quad W \tag{2.35}$$

$$\text{subject to} \quad W < W_d, d \in \mathcal{R} \tag{2.36}$$

$$W_d = \sum_{j \in N_1} f^d_{j,1} - \sum_{j \in N_1} f^d_{1,j}. \tag{2.37}$$

$$\sum_{j \in N_i} f^d_{j,i} - \sum_{j \in N_i} f^d_{i,j} = 0, i \neq 1, d \tag{2.38}$$

$$0 \leq f^d_{i,j} \leq t_{i,j} z_{i,j} \tag{2.39}$$

$$\sum_{j \in N_i} t_{i,j} < 1 \tag{2.40}$$

$$t_{i,j} > 0 \tag{2.41}$$

$$z_{i,j} = \lambda_i \cdot \left(1 - Q\left(\sqrt{\frac{P^{\text{Tx}}_i \cdot h_{ji}}{\sum_{m \neq j,i}(P^{\text{Tx}}_m \cdot h_{jm}/g_i) + \sigma^2}}\right)\right)^l \tag{2.42}$$

$$\text{variables} \quad f^d_{i,j}, t_{i,j}, W_d, \forall (i,j) \in E, d \in \mathcal{R}; \mathbf{P}^{\text{Tx}}, W.$$

In equation (2.42), h_{ji} is the link gain and g_i is the processing gain. Feeding this formulation with the same topology and initial conditions as that are used in the dynamic power control simulation, a numerical nonlinear program solver yields the optimal value of 1pkt/ms with Sequential Quadratic Programming (SQP) method [28]. However, note that this algorithm can only be applied in a static fashion, i.e., it does not retain the dynamic characteristics of the power control in equation (2.16). Without taking into account the dynamic growth of ranks in RNC, any changes in the network would render a previously optimal allocation unsatisfactory and to make it work, a new allocation has to be computed.

Online algorithm

In the simulation for online power control, the power is adjusted in every discrete time interval. Here, the interval is set to 150ms. The power levels of all the nodes are set to 13dBm in the first interval, and a random update is applied in the second interval. After this initialization, in any interval n, we attempt to maintain a fixed step size γ with the following rule:

$$P_i^{\mathrm{Tx},n} = \begin{cases} P_i^{\mathrm{Tx},n-1} + \gamma, & \text{if } a \cdot B_i'(\mathbf{P}^{\mathrm{Tx},n-1}) \geq \gamma \\ P_i^{\mathrm{Tx},n-1} - \gamma, & \text{if } a \cdot B_i'(\mathbf{P}^{\mathrm{Tx},n-1}) \leq -\gamma \\ P_i^{\mathrm{Tx},n-1}, & \text{otherwise.} \end{cases} \tag{2.43}$$

In this simulation, we set γ as 0.2dBm. From Figure 2.7(a), we can see in the first interval of this experiment, the destination nodes' largest throughput is about 0.5pkt/ms, and the throughputs of node 4 and 5 are both less than 0.3pkt/ms. As the algorithm progresses, the minimum throughput increases from about 0.1pkt/ms to about 1pkt/ms, and approaches convergence of about 1pkt/ms around $t = 1500$ms. Figure 2.7(b) shows how the transmit powers at each node are adjusted by the online power control algorithm.

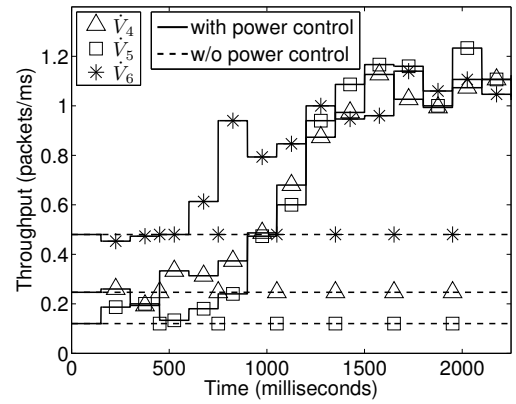

(a) Effect of power control on throughput

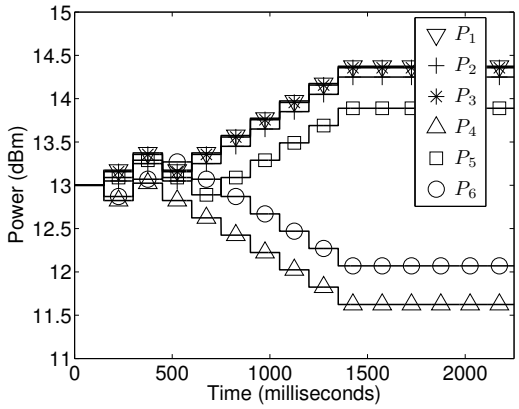

(b) Power adjustment

Figure 2.7: Online power control (a) Throughput, (b) power adjustment.

2.5 Dynamic CSMA Mean Backoff Delay Control in RNC

We now consider another resource allocation problem for RNC at the MAC layer, namely, CSMA mean backoff delay control. There exist a number of algorithms for maximizing CSMA throughput by link scheduling in a multihop network, as can be found in [29–31]. However, these algorithms do not consider or make use of the broadcast effect of wireless transmissions as RNC does. When CSMA is the underlying wireless media access control mechanism of a coded packet network, we perform dynamic CSMA backoff time control to optimize network coding performance, taking into account that each transmission is intrinsically a broadcast and neighbors will receive

the transmitted packet. Although the general algorithm presented in section 2.3 is sufficiently flexible such that it does not need to assume any particular model for λ_i, we now introduce a CSMA model for the purpose of illustration. We then apply the resource allocation algorithm in this setting to dynamically adjust the mean of backoff delay at each node to maximize the minimum throughput among the sink nodes. Note that the differential equation framework in equation (2.5) described earlier requires the knowledge of $z_{i,\mathcal{K}}$, the rate at which the packets from i are successfully received by at least one node in $\mathcal{K}$. We will now derive $z_{i,\mathcal{K}}$ for this CSMA model.

2.5.1 CSMA Model

The CSMA model considered here was first introduced in [32] and is illustrative of a multihop network as is the case for RNC. We consider the wireless network $G = (\mathcal{N}, \mathcal{E})$ and let N_i denote the neighbors of node i, i.e., all the nodes that are within the range to be able to communicate with node i and $N_i^* = N_i \cup \{i\}$. It should be noted that we assume here that the layer of network coding operation sits above the MAC layer on the protocol stack, and in this section, we refer to *packet* as the coded packet with the MAC header attached. We describe next the assumptions for the CSMA model from [32]:

- When a packet is scheduled to be transmitted at node i, the node senses the channel first. If the channel is idle, i.e., no ongoing transmissions from N_i, node i transmits the packet immediately. We assume that the packet length is exponentially distributed with instantaneous transmission (zero propagation delay). We use $1/\mu_i$ to denote the mean of node i's packet length.

- After sensing the channel, if the channel is busy, node i defers its transmission according to a random delay. The scheduling of packets, including the deferred ones, together with the newly scheduled after a successful transmission, is a Poisson process with rate α_i.

- Any node from N_i, which are not currently receiving, can receive the packet from

node i without error immediately after the transmission. Subsequent transmissions heard by node i while it is receiving will fail.

Let $x^i, i = 0, 1, ..., M$ be a length-N vector denoting the valid transmission status of the whole network where the jth component of x^i, x^i_j, is 1 if node j is transmitting, and 0 otherwise. For instance, [1 0 0 1 0 0] implies node 1 and node 4 are transmitting and other nodes are idle, and it is only valid when node 1 and 4 are not neighbors of each other. Let $G(x^i)$ denote the set of transmitting nodes in state x^i and $H(x^i)$ denote the set of nodes that are not neighbors of any node in $G(x^i)$. The state transitions among all the states x^i constitute a finite-state continuous Markov chain. Let $Q(x^i)$ be the stationary probability of state x^i, we have the following global balance equations:

$$\begin{aligned} &\textstyle\sum_{j\in G(x^i)} Q(x^i)\mu_j + \sum_{j\in H(x^i)} Q(x^i)\alpha_j \\ &= \textstyle\sum_{j\in G(x^i)} Q(x^i - \mathbf{e}_j)\alpha_j + \sum_{j\in H(x^i)} Q(x^i + \mathbf{e}_j)\mu_j,\ i = 1, ..., M, \end{aligned} \tag{2.44}$$

where $\mathbf{e}_j$ is a length-N vector where the jth component is 1 and 0's elsewhere. It can be verified that the following detailed balance equations hold:

$$Q(x^i + \mathbf{e}_j)\mu_j = Q(x^i)\alpha_j, \quad i = 0, 1, ..., M, j \in H(x^i). \tag{2.45}$$

Let x^0 denote the state that no nodes are transmitting, and define $v_j = \alpha_j/\mu_j$. Then

$$Q(x^i) = Q(x^0) \prod_{j\in G(x^i)} v_j, \quad i = 1, ..., M, \tag{2.46}$$

and

$$Q(x^0) = 1/(\sum_i \prod_{j\in G(x^i)} v_j). \tag{2.47}$$

Note that for a packet scheduled by node i to be received by one of its neighbor nodes, j, the following requirements must be satisfied:

- i must be idle.
- All the neighbors of i, including j, must be idle.
- All the neighbors of j must be idle.

Based on the above results from [32], we can now proceed to derive the probability that a packet scheduled by node i can be received by a neighbor node j and let $P'_{i,j}$ denote this probability. One should distinguish $P'_{i,j}$ from $P_{i,j}$, since $P_{i,j}$ is the conditional probability that a packet *transmitted* by node i can be received by node j. Let $I(X)$ denote the event that all the nodes from the set X are idle. Then

$$P'_{i,j} = \text{Prob}[I(N_i^* \cup N_j^*)] = \sum_{G(x^m) \subset \mathcal{N} \setminus (N_i^* \cup N_j^*)} Q(x^m). \tag{2.48}$$

Further, we continue to derive $P'_{i,\mathcal{K}}$, the probability that a *scheduled* packet from i can be received by at least one node in $\mathcal{K}$. Let $\mathcal{K}' = \mathcal{K} \cap N_i$, then

$$P'_{i,\mathcal{K}} = P'_{i,\mathcal{K}'} = \sum_{\exists \mathcal{A} \subset \mathcal{K}', \text{ s.t. } G(x^m) \subset \mathcal{N} \setminus (N_i^* \cup N_{\mathcal{A}}^*)} Q(x^m), \tag{2.49}$$

where $N_{\mathcal{A}}^* = \cup_{i \in \mathcal{A}} N_i^*$. Then, the rate at which node i's packets are successfully received by at least one node from set $\mathcal{K}$ is given by:

$$z_{i,\mathcal{K}} = \alpha_i P'_{i,\mathcal{K}}. \tag{2.50}$$

While the above developments assumed that packet length is exponentially distributed, it turns out that this assumption can be relaxed. For instance, it has been shown in [33] that the results derived using the above model are more sensitive to the mean μ_i, rather than the distribution itself. Therefore, the expressions in equations (2.49) and (2.50) are suitable for analyzing CSMA in a RNC network where transmitted data packets at the network layer are assumed to be of the same length.

2.5.2 Centralized Gradient Algorithm for CSMA Mean Backoff Delay Control

In a CSMA network, we consider the network resource $\mathbf{r}$ to be the rate of the Poisson scheduling process, $\boldsymbol{\alpha}$, i.e., $\mathbf{r} = \boldsymbol{\alpha}$. Since a Poisson process has exponentially distributed arrival times, the backoff delay of node i will be exponential with mean $1/\alpha_i$. Our goal is to adjust $\boldsymbol{\alpha}$ to maximize the minimum throughput. Thus, as long as we have the formulation of the CSMA model above, we know that the reception rate $z_{i,\mathcal{K}}$ is a function of $\boldsymbol{\alpha}$, i.e.,

$$z_{i,\mathcal{K}} = z_{i,\mathcal{K}}(\boldsymbol{\alpha}). \tag{2.51}$$

Let node k be the node with the minimum throughput among all the destination nodes, i.e., $k = \arg\min_{j\in\mathcal{R}} \dot{V}_j$. Then based on the system of equations (2.5), we have:

$$\begin{aligned}\dot{V}_k &= \textstyle\sum_{i\in N_k} z_{i,k}(1 - q^{V_k - V_{\{i,k\}}}) \\ &= \textstyle\sum_{i\in N_k} \alpha_i \cdot \left(\sum_{G(x^m)\subset\mathcal{N}\setminus(N_i^*\cup N_k^*)} Q(x^m)\right) \cdot (1 - q^{V_k - V_{\{i,k\}}}) \\ &= \textstyle\sum_{i\in N_k} \alpha_i \cdot \left(\sum_{G(x^m)\subset\mathcal{N}\setminus(N_i^*\cup N_k^*)} Q(x^0)\prod_{j\in G(x^m)} \alpha_j/\mu_j\right) \cdot (1 - q^{V_k - V_{\{i,k\}}}).\end{aligned} \tag{2.52}$$

The versatility of the aforementioned dynamic resource allocation algorithm allows us to derive an algorithm customized for the CSMA backoff delay control problem. To this end, we follow equation (2.10) and get

$$\dot{\alpha}_i = a \cdot \left(\dot{V}_k(\boldsymbol{\alpha} + \Delta v \mathbf{e}_i) - \dot{V}_k(\boldsymbol{\alpha})\right), \tag{2.53}$$

where a is the control gain value, Δv is the step size, and $\mathbf{e}_i$ is a vector whose ith component is 1 with 0 elsewhere. We define an ascent direction vector $\mathbf{B}(\boldsymbol{\alpha})$ such that its ith component is given by:

$$B_i(\boldsymbol{\alpha}) = \dot{V}_k(\boldsymbol{\alpha} + \Delta v \mathbf{e}_i) - \dot{V}_k(\boldsymbol{\alpha}). \tag{2.54}$$

Then the centralized backoff delay control algorithm can be written in the following iterative form:

$$\boldsymbol{\alpha}^n = \boldsymbol{\alpha}^{n-1} + a \cdot \mathbf{B}(\boldsymbol{\alpha}^{n-1}). \tag{2.55}$$

2.5.3 Online Gradient Algorithm for CSMA Mean Backoff Delay Control

We can also derive an online version of the resource allocation algorithm for CSMA mean backoff delay control based on the centralized gradient algorithm. As in the case of dynamic power control, the online algorithm for CSMA backoff control at each node makes the estimation of the gradient, denoted by $\mathbf{B}'(\boldsymbol{\alpha})$, i.e., $\mathbf{B}'(\boldsymbol{\alpha}) \approx \nabla_{\mathbf{z}'}\dot{V}_k$ without the demand of knowing the underlying PHY/MAC layer specifics at other nodes; rather, the estimation is based on a limited amount of network state information, obtained through message exchanges. Specifically, during each interval n, we seek an estimation of the gradient given as follows:

$$\mathbf{B}'(\boldsymbol{\alpha}^n) = \nabla^n_{\mathbf{z}'}\dot{V}_k \hat{J}^n_{\boldsymbol{\alpha}}\mathbf{z}'. \tag{2.56}$$

where $\boldsymbol{\alpha}^n$ is $\boldsymbol{\alpha}$ at the nth time interval and $\hat{J}^n_{\boldsymbol{\alpha}}\mathbf{z}'$ is an estimation of the Jacobian of $\mathbf{z}'$ with respect to $\boldsymbol{\alpha}$ during the nth interval. In the above equation, $\nabla^n_{\mathbf{z}'}\dot{V}_k$ could be readily obtained in a similar way as for online power control (see equations (2.26) and (2.27)). Further, the estimation of Jacobian, $\hat{J}^n_{\boldsymbol{\alpha}}\mathbf{z}'$ for the nth interval, could be obtained by following Broyden's method [26]:

$$\hat{J}^n_{\boldsymbol{\alpha}}\mathbf{z}' = \hat{J}^{n-1}_{\boldsymbol{\alpha}}\mathbf{z}' + \frac{\Delta\mathbf{z}'^n - \hat{J}^{n-1}_{\boldsymbol{\alpha}}\mathbf{z}'\Delta\boldsymbol{\alpha}^n}{\|\Delta\boldsymbol{\alpha}^n\|^2}\Delta\boldsymbol{\alpha}^{n\top}. \tag{2.57}$$

where $\Delta\boldsymbol{\alpha}^n = \boldsymbol{\alpha}^n - \boldsymbol{\alpha}^{n-1}$. With the estimated ascent direction $\mathbf{B}'(\boldsymbol{\alpha})$ being established, we can write the following iterative method to adjust the value of the mean backoff delay:

$$\boldsymbol{\alpha}^n = \boldsymbol{\alpha}^{n-1} + a \cdot \mathbf{B}'(\boldsymbol{\alpha}^{n-1}), \tag{2.58}$$

2.5.4 Numerical Results

We perform two kinds of evaluations: (i) a differential equation solver based evaluation for centralized CSMA mean backoff delay control and (ii) an event-driven simulation for the online algorithm. We use the 6-node network shown in Figure 2.1 and consider that each node has a set of neighbor nodes, as summarized in Table 2.1. The neighbors are determined based on a thresholding distance between nodes.

Node	Neighbors
1	$\{3, 5\}$
2	$\{5, 6\}$
3	$\{1, 4, 5\}$
4	$\{3, 5, 6\}$
5	$\{1, 2, 3, 4, 6\}$
6	$\{2, 4, 5\}$

Table 2.1: Nodes and their neighbors.

Recall that α_i is the scheduling rate of node i. We measure this rate in packets per millisecond (pkt/ms). In both evaluations, we introduce a scalar parameter β_i taking the value of $\log 1000\alpha_i$. We call β_i the transmission aggressiveness of node i and set

$3 \leq \beta_i \leq 6.5, i = 1, 2, ..., N$. Initially, β_i of every node i is set to 4 and therefore the average scheduling rate α_i is about 0.06pkt/ms. We assume the packets are of fixed length and set $1/\mu_i$ of any node i to be 1/1000ms.

Centralized algorithm

The results of DE solver based evaluation for centralized CSMA mean backoff delay control is shown in Figure 2.8. The dashed lines in Figure 2.8(a) indicate that without dynamic backoff control, the throughput of nodes $4, 5, 6$ remain at about 0.06pkt/ms. The resource allocation algorithm increases all the three destination nodes' performance and their throughputs converge to about 0.22pkt/ms, making it a gain of greater than 200% from the initial throughputs. Figure 2.8(b) shows how the transmission aggressiveness β is continuously adjusted at each node.

Online algorithm

From Figure 2.9(a), we can see that all the three destinations' original throughputs are less than 0.075pkt/ms at $t = 0$ms. Starting from $t = 1$ms, the online resource allocation algorithm gradually improves the throughputs of all the destination nodes. Around $t = 7000$ms, the throughputs begin to converge around 0.20pkt/ms. Figure 2.9(b) shows how the transmission aggressiveness is adjusted by the online algorithm.

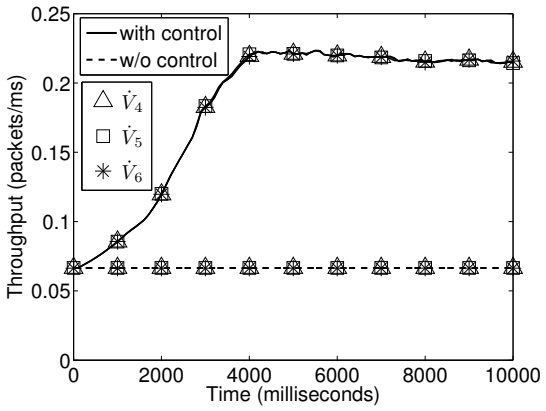

(a) Effect of contention window size control on throughput

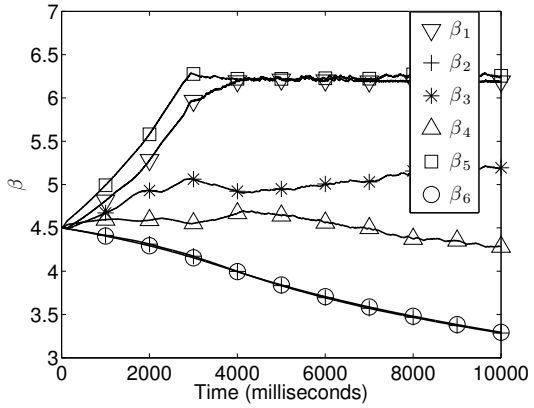

(b) Contention window size adjustment

Figure 2.8: Centralized contention window size control (a) Throughput, (b) contention window size adjustment.

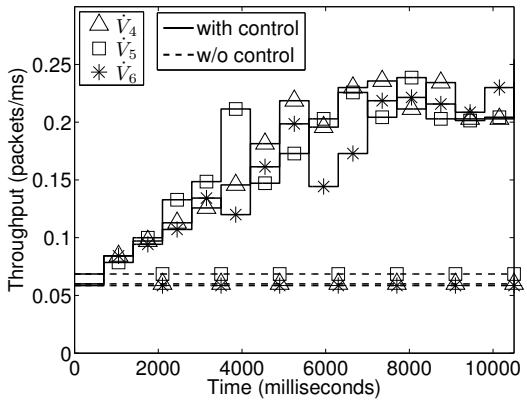

(a) Effect of contention window size control on throughput

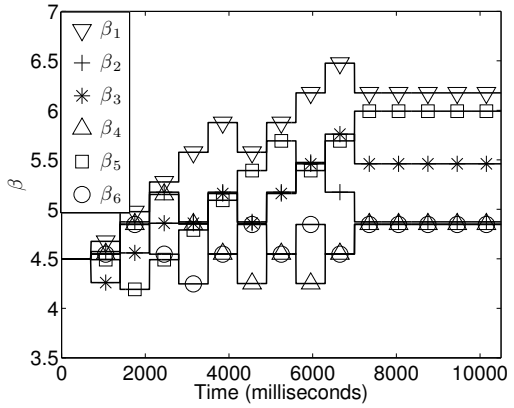

(b) Contention window size adjustment

Figure 2.9: Online contention window size control (a) Throughput, (b) contention window size adjustment.

Chapter 3

Transport protocols for MobilityFirst future Internet architecture

3.1 Introduction

The TCP/IP architecture underpinning the current Internet is based on the end-to-end principle [34] of minimizing functionality in the network while handling service-specific requirements such as error and flow control at the end-points. In addition, the current Internet architecture is based on the concept of routing between IP addresses requiring a static one-to-one association between hosts and network locators. While the Internet works well for traditional kinds of communication, emerging mobile content and Internet-of-Things (IoT) services have motivated consideration of clean-slate *Information-Centric Network* (ICN) architectures [35,36] which operate on names rather than addresses. Several distinct architectures for ICN have recently been proposed including MobilityFirst (MF) [37, 38], Named Data Network (NDN) [39], and XIA [40]. While there are differences in detail, all the proposed ICN protocols share some common design elements that need to be considered in the design of transport protocols to be used for end-to-end services. Specific characteristics of ICN include: (a) use of names to identify sources and sinks of information; (b) storage of information at routers within the network in order to support content caching and disconnection; (c) multicasting and anycasting as integral network services; and in the MF case (d) hop-by-hop reliability protocols between routers in the network. These properties have significant implications for transport protocol design since the current protocols, TCP and UDP, were designed based on the end-to-end Internet principle, which typically assumes end-to-end connectivity during a transfer and uses address based routing with

minimal functionality (i.e., no storage or reliability mechanisms) within the network.

Consider first the implications of name-based routing on transport protocol design. Communication with named objects, whether content files, devices, groups of devices or more complex context-based groups is different from conventional TCP connections in the sense that an object may have multiple end-points because the object may be multi-homed (i.e., multiple network interfaces to the same device) or multicast (to multiple devices, each with a different network interface) or multi-copy (i.e., multiple instances of the same information object can be found at different places in the network). This indicates that transport protocols need to be designed to provide appropriate service semantics for retrieving or delivering such named objects, for example, in multicast where the information object reaches all the named destinations or anycast where the object is fetched from the "nearest location". A second important property of ICN protocols is the fact that routers may store information objects such as content either for caching or for delay tolerant delivery. This implies the existence of in-network transport proxies which are in between the source and the destination, and the transport protocol should be designed to take advantage of the in-network copy to provide the desired service efficiently. For example, reliable delivery with an ICN transport would be able to utilize a copy of the information object stored at an intermediate router and avoid the need for end-to-end retransmission used in TCP. The third feature of ICN architectures is the fact that in-network storage can be associated with reliable hop-by-hop transmission of information objects between routers, thus alleviating the need for strong reliability mechanisms at the transport layer depending on the type of service desired.

In Section 3.2, we consider the requirements for ICN transport in further detail and identify a set of core transport protocol functions needed to address an anticipated range of service requirements. These core transport protocol components are developed in further detail for a specific ICN architecture, MobilityFirst, and several examples of how these functions are integrated with the named-object network layer are given in Section 3.3. The prototype of MFTP is discussed in Section 3.4. Then we provide a set of experimental results based on the prototype and compare its performance with

conventional TCP/IP to the extent possible.

Our contributions in designing and implementing transport protocols for an ICN architecture with explicit locators, such as MF, are twofold: (i) we examine a representative set of delivery service scenarios, and based on them, define the requirement space for transport protocols for any Information Centric architecture; (ii) with explicit locators in an ICN architecture, much richer end-to-end semantics, such as reliability delegation, and in-network retransmission, are enabled by integrating in-network transport services. We show that such features are conducive to supporting mobility, and flexibly and robustly supporting different delivery patterns. The proposed design is validated using an experimental prototype, with bulk (e.g., video) content and latency-sensitive web (text, image and video) content delivered over wireless networks to mobile clients. The general principles of our design for end-to-end transport, regardless of whether MF-like locators are used, can also be customized to work with and bring benefits to NDN as well, e.g., to apply per-hop error and congestion control to improve transmission efficiency, and employ router-proactive mechanisms to provide better and richer mobility support.

3.2 Requirements for transport layer service for ICN

We analyze four common service scenarios, and identify the set of transport layer features for an ICN environment (see the summary of requirements in Table 3.1).

Large file retrieval. A large file retrieval is abstracted as a *get*(content_name) socket call [41] in an ICN context. Clients inject a content request, independent of the content location, with a *get*() call, and the network will route the request to the location of a copy of the content. Then a flow with a large volume which carries the content is transferred reliably from the server to the requesting client. This is often referred as *anycast*.

Key TP functions required: Because of the large amount of data to be delivered, file transfer requires: (i) fragmentation and sequencing at the source, and reassembly at

Service scenarios	Fragmentation and resequencing	Reliable delivery	Lightweight transport	Flow and congestion control	In-network proxy
Large file retrieval	✓	✓		✓	✓
Web content retrieval	✓	✓		✓	
M2M communications	✓		✓		✓
Multicast	✓	✓	✓	✓	✓

Table 3.1: Transport requirements for different service scenarios

the sink; (ii) efficient usage of network resources with source rate control so as not to introduce congestion. The imbalance of rates at different segments of an end-to-end path makes it difficult to perform end-to-end control at high speeds, with small amounts of buffering, and to deal with transient disruptions. This problem can be alleviated by providing additional in-network transport services, such as temporary storage for in-transit data (we call the en-route node with transport services a *transport proxy*).

Web content retrieval. In a web-browsing application, a sequence of content requests are sent by the client to the server. Each of the requests is for retrieving a constituent named object of a webpage. Two characteristics are inherent in web content retrieval: i) these requested objects are generally small in size, i.e. of tens or hundreds of kB; ii) user experience dictates that the objects must be received in a timely manner, preferably no more than several hundred milliseconds, thus making the transfer latency-sensitive. *Key TP functions required:* End-to-end error and congestion recovery need to be provided, but in a lightweight manner, because any significant setup overhead is not amortized easily. Flow control is not required due of the limited amount of data transmitted,

in order to avoid unnecessary overhead contributing to increased latency.

M2M communications. In Machine-to-machine (M2M) communications, sensor data by nature is idempotent. That is, if the PDU is lost (due to bit errors or congestion) or it is delayed beyond the limits of latency for the data, the transport layer need not attempt to reliably deliver that PDU. This transfer paradigm is captured in a *send*(dst_name, content_name) API with no explicit reliability preference.
Key TP functions required: In such cases, the transport layer could simply resort to stateless communication (e.g., lightweight transport with no error recovery and no flow/congestion control) to minimize overheads. Moreover, due to power constraints in devices, a sensor node may not be on all the time. End-to-end control is not always possible in this case and delegation of transport service guarantees, such as reliability, need to be made to other en-route nodes. Thus in-network proxy support is desired.

Multicast. A number of popular applications are based on multicast, such as group-based subscriptions (RSS), teleconferencing, online gaming, etc. In a name-based architecture, multicast can be realized with a *send* (dst_name, content_name) API with the dst_name referring to a group of individual endpoints names.
Key TP functions required: Guaranteeing 100% reliability in a multicast session is a well-known hard problem. To achieve reliable transport, the source relies on negative acknowledgement (NACK) from clients to initiate retransmissions. With the number of subscribers increasing, retransmission has to be implemented in an efficient manner such that the ACK-implosion (see [42]) is avoided. This may require aggregation of retransmission requests in the network, and retransmission from within the network. Thus in-network proxies are desired to handle such aggregation and storage of pieces of contents for retransmission.

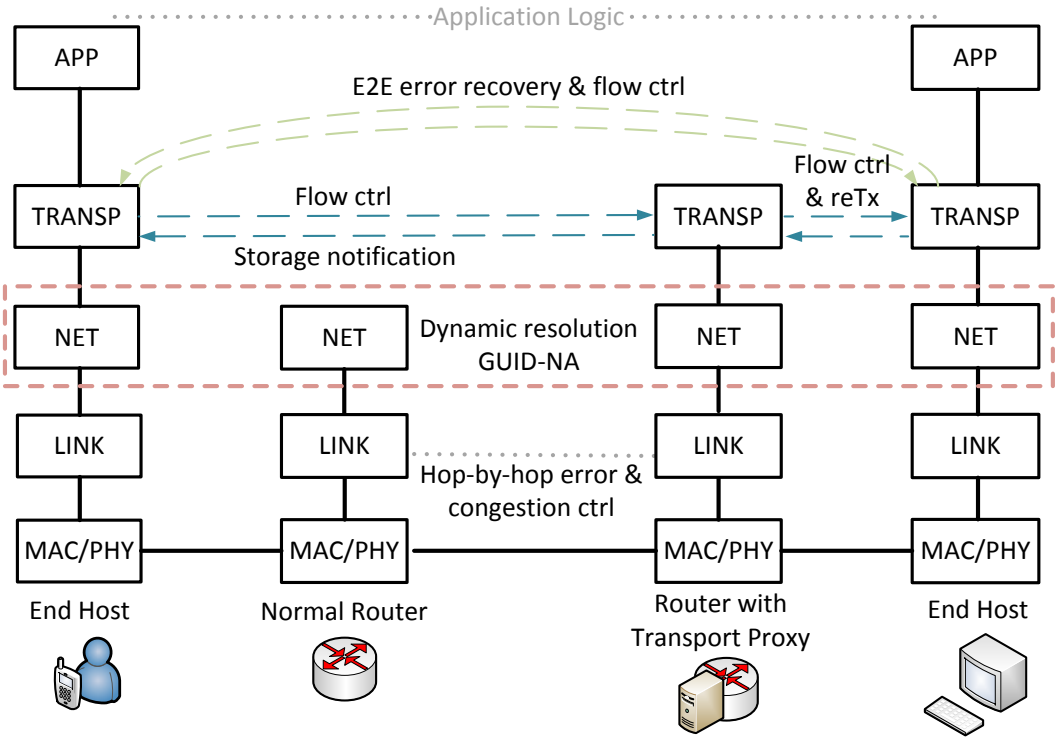

Figure 3.1: Protocol stack and transport layer functionalities

3.3 MFTP design

MFTP is based on the four characteristics of different ICN proposals to support the analyzed requirements. Specifically, MFTP has been designed to operate on top of the MobilityFirst networking stack [43, 44], while the principles may be more broadly applicable to other ICN frameworks. As described in [38], MobilityFirst is based on a clean separation of names and network addresses with a logically centralized but physically distributed global name resolution service (GNRS). The globally unique identifier (GUID) in MF is a flat public key identifier, i.e. a name, which can be used to represent any network attached object, including devices, people, groups, content, or context. Fig. 3.1 shows the major layers in the MF protocol stack and the role of the MFTP transport layer above the named-object GUID based network layer which is supported by the GNRS [44,45]. For additional details on MF, the reader is referred to [38,41,43,44].

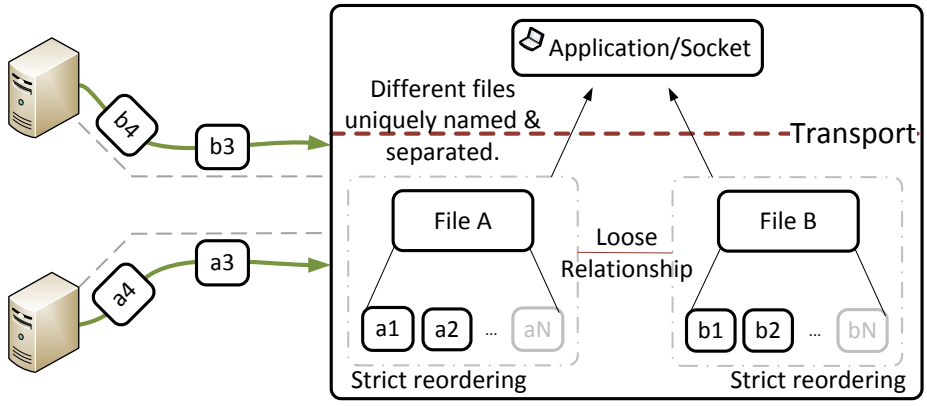

Figure 3.2: Illustration of named object's implication to fragmentation and sequencing. Transport layer fragments a content into large chunks. Sequential delivery is guaranteed for each content, but no strict ordering maintained for chunks of different contents.

3.3.1 Segmentation and re-sequencing

Typically in ICN, a data request is abstracted by an API, *get*(content_name). In NDN, such a request, called an Interest, with an associated relative sequence number, solicits one segment of a content. In MF, the requestor only sends one request for a piece of content; the server that handles the request then segments the content and assigns the segments a relative sequence number. In any case, sequence numbers are bound to the named content, rather than the two endpoints. This has significant implication for the hop-by-hop transfer and storage capability in ICN, as we shall see later. With content-centricity, such a sequencing scheme works naturally for anycast, multicast and multipath transfers. For example, in an anycast scenario, the forwarding plane decides

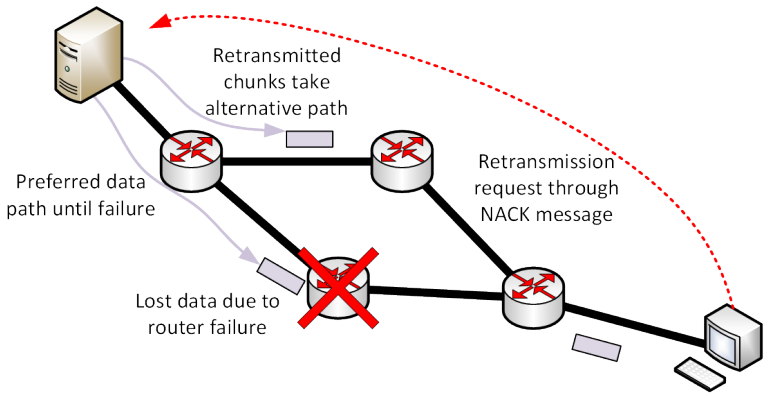

Figure 3.3: End-to-end signaling to recover from in-network failure

where the content request should be handled. The transport layer is oblivious of the server location; rather, the transport's functionality of providing ordering and reliability can be fulfilled based on the knowledge of the data being delivered, using the content names and sequence numbers.

On the sender side, the transport layer segments the application data into large chunks, whose size can be negotiated by the two end-points based on a tradeoff between the overheads and the fair use of network resources across flows. We allow the chunk size to go up to the order of megabytes.The link layer still logically maintains the semantics of a "chunk" at each hop. Figure 3.2 illustrates how the transport layer would support concurrent reception of multiple files. As shown in the figure, in-order delivery is strictly enforced among the chunks of a single transported file: transport will buffer out-of-order chunk arrivals. Only a loose relationship is maintained across multiple files, because each file has a unique name and there is no need for strict ordering of delivering the received content based on the order of the requests, regardless of where the files originate.

3.3.2 Coordinated End-to-end error recovery and hop-by-hop reliable delivery

In traditional transport protocols such as TCP, detection of loss (whether due to errors or congestion) or congestion at a link is communicated to the sender after a feedback

delay, possibly quite a few end-to-end RTT's. After the detection, recovery mechanisms, such as congestion recovery or retransmission, can incur an unduly large penalty to the flow. Also, due to queuing at routers, and heterogeneous transmission technologies employed along the route to destination, spurious, or premature, retransmissions are not uncommon [46]. Link level mechanisms alleviate these problems as errors can be detected and reacted upon more quickly. Hop-by-hop transfer is suitable in ICN due in part to the fact that the segment of data being transferred is named; moreover, ICN routers can have storage capability, and can temporarily store the in-transit copy to provide delay-tolerant delivery, and also cache a copy to serve future requests. In NDN, each named data item is indeed transferred in a hop-by-hop manner: upon receiving such a data item, the router examines whether an Interest for the data has been received earlier, and whether it needs to cache the data.

MFTP integrates per-hop error recovery and congestion control whenever the problem can be resolved locally, and only invokes end-to-end mechanisms when it is absolutely necessary, e.g., a router fails and loses all the buffered data. On each hop, after every chunk that is transmitted, a corresponding control message called *CSYN* is used to explicitly request acknowledgement from downstream, which then replies with a bitmap of reception status for every packet in that chunk. The transmission for this chunk finishes if there is no loss, otherwise the lost packets of that chunk are retransmitted locally following the same procedure until all packets are received.

Taking advantage of the hop-by-hop reliability of the network, we seek to have a parsimonious end-to-end mechanism that has minimal overhead. The end-to-end error recovery mechanism is built to be *flexible* to accommodate application and sender needs (including *don't care, NACK, ACK*). With a Negative-ACK, i.e. NACK, the transport reduces end-to-end message overhead, and the receiver provides notification only when a chunk is not delivered over a conservatively long period of time (as a result of a failure that causes the reliable hop-by-hop mechanism to lose an acknowledged chunk as shown in Figure 3.3). It is only for short-sessions (e.g., single PDU delivery) and for latency-sensitive interactions that the sender would enable the use of an end-to-end ACK option. With idempotent data transmissions (e.g, sensor data which the transport

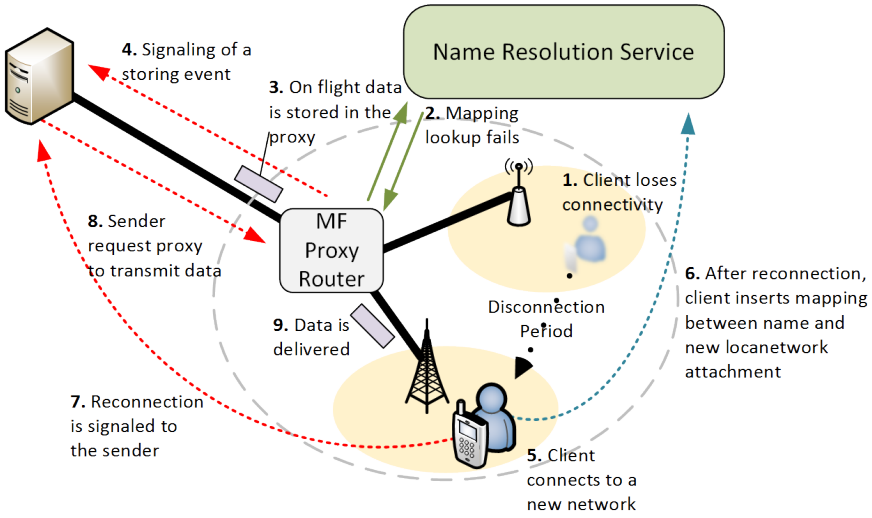

Figure 3.4: Procedures involved to use in-network transport proxy to handle destination disconnection and retransmission: the proxy temporarily stores chunks when the destination disconnects, and transmits to the client when connectivity is restored as indicated by the name resolution service.

layer sends and forgets), the sender may choose to use the *don't care* option.

3.3.3 In-network transport proxy

One of the challenges for conventional transport protocols is in dealing with the content delivery to mobile devices, where mobility results in intermittent connectivity and the end-to-end connection experiences frequent disruptions. If the transport protocol has to re-establish the connection, then the transfer has to re-start and any data already in transit in the network will have to be discarded. ICN's architecture inherently supports mobility and resolves connection disruptions in multiple ways. For instance, in NDN, each data is solicited by an Interest packet; in case a client moves before obtaining the requested data, it can re-issue an Interest packet for the same data, which will be delivered to the new location. In the MF architecture, the network can take on a more proactive role in re-initiating data transfers when connectivity is re-established.

To this end, we postulate having routers (or at least a subset of them) which provide

in-network transport service such that the original source can delegate part of the end-to-end data transfer responsibility. The router, which we call an *in-network transport proxy*, would have substantial amounts of memory, e.g., several GB, to temporarily hold in-transit chunks when the destination is unreachable. This disruption may be due to: lack of connectivity to a mobile destination node, until connectivity is subsequently re-established; alternatively, in M2M communication, when a sensor node is only powered on intermittently, it may choose to deliver information chunks to the next hop and then power down.

The mechanisms implemented by such a node are shown in Figure 3.4: when faced with the impossibility of forwarding chunks with the information available at the network layer (i.e. the router detects that connectivity towards the destination of a chunk is disrupted), the router pushes up to the transport proxy layer the relative data chunks. Two reasons might generate this impossibility of forwarding chunks: (i) the destination does not have an active network address (NA) binding corresponding to its GUID entry in the GNRS; (ii) the chunk reaches the destination network given by its most recent binding, but either the destination has changed its point of attachment or it has disconnected from the network before the previous NA entry expires in the GNRS server. As a consequence, the link layer is not able to deliver the chunk despite several attempts, and corresponding CSYN timeouts. In these cases, the chunk is pushed up to the proxy layer to be temporarily stored. While this is similar to Delay-Tolerant Network protocols, the innovation here is the integration of these mechanisms with the support of dynamic mobility and ICN style named object services.

We limit the amount of content that can be stored for a flow. Each (source GUID, destination GUID) pair is limited to have buffered content up to size S. When a chunk for a new flow arrives, the chunk will be stored directly if sufficient space is available for the new flow; otherwise, a chunk for the oldest flow is replaced from the storage by the new chunk. When the chunk is stored, a timer is created to schedule future transmission. Further, a transport layer message, either *Store* or *Drop*, is transmitted back to the original source to notify it of the intermediate proxy storing or dropping the chunk. A stored chunk will be scheduled to retry a GNRS lookup to bind an updated

NA to the destination GUID when its storage timer expires. The chunk will be pushed out if an NA is found, i.e., destination becomes connected again, otherwise it will be kept in storage. On the other hand, rescheduling of the chunks can also be initiated by the original source of a chunk. As is shown in Fig. 3.4, when the source receives a NACK message identifying a chunk as missing, if it is aware that the corresponding chunk originally destined to the requesting destination is stored in the network, based on a previously received *Store* message, it utilizes this in-network copy and initiates the retransmission from inside the network. This is done by the source sending a *Push* message to the in-network proxy to trigger retransmission.

Transport proxies also support content producer mobility by allowing the producer to delegate its end-to-end reliability guarantee to the proxy. For instance, a mobile client intending to upload a recently shot video can specify in the pushed data chunk that such a delegation is requested. Before forwarding the data chunk, the immobile access router (acting as a transport proxy) will save a copy of the chunk in order to respond to potential future NACKs.

3.3.4 Flow control and congestion control

MFTP uses a combination of per-hop back-pressure for congestion control and end-to-end window-based flow control.

Hop-by-hop congestion control: The hop-by-hop back-pressure scheme is built on top of a back-pressure buffer (of capacity B packets).As illustrated in Fig. 3.5, the back-pressure buffer essentially has all the chunks that are received from the network and are queued to be transmitted. In addition, between two adjacent routers on a link, the sender maintains a sending window W_{ostd}, i.e., number of outstanding packets, that is bounded by the receiver's advertised window, W_{ad}. Following the transmission of a chunk of data, a CSYN message is sent, which the downstream node then acknowledges with a CACK message. The number of outstanding packets, W_{ostd}, is reduced based on the downstream node's acknowledgement. When the occupancy of back-pressure buffer reaches its capacity, the router throttles the advertised window to all of its upstream nodes. This "congestion signal" eventually propagates back to the original

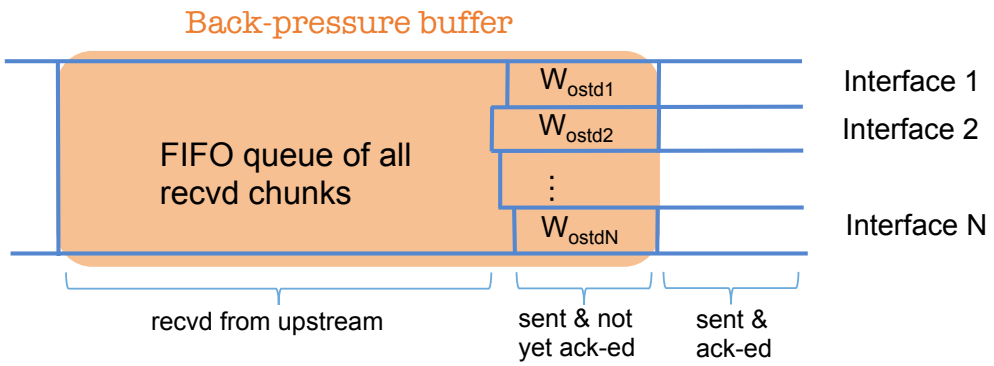

Figure 3.5: Back-pressure buffer and per-hop sending window.

traffic sources in a hop-by-hop manner, thus eventually limiting the traffic injected into the network.

End-to-end flow control: Hop-by-hop back-pressure is not sufficient to prevent the receiver's buffer from being overrun by the sender's data from an end-to-end perspective. Because MFTP does not require the receiving side to send frequent reception status update in the reverse path (it depends only on NACKs), the feedback from the receiver is both parsimonious and not timely for the sender to detect receiver buffer overflow. We therefore consider an explicit notification from the receiver. The sender starts at a initial end-to-end sending window W_e. For each window's worth of data chunks, the receiver then sends one window flow control message, to advise the sender to maintain, increase, or reduce the sending window to certain value based on the receiver's buffer occupancy. This message will be delivered reliably to the sender. Note that the sending window is also the atomic unit for the end-to-end NACK message, thus the NACK and flow control are fulfilled by a single message (if a NACK has to be sent, i.e., some chunks are lost). In the event that this special chunk is lost due to a node failure, a NACK timeout at the receiver would trigger the receiver to proactively notify the sender of the reception status (NACK) and receiver buffer status (flow control).

Small content transfers are not subject to such end-to-end flow control, mainly because the transfer will be complete even before the flow control notification can be generated. However, small content transfers are still regulated by per-hop congestion

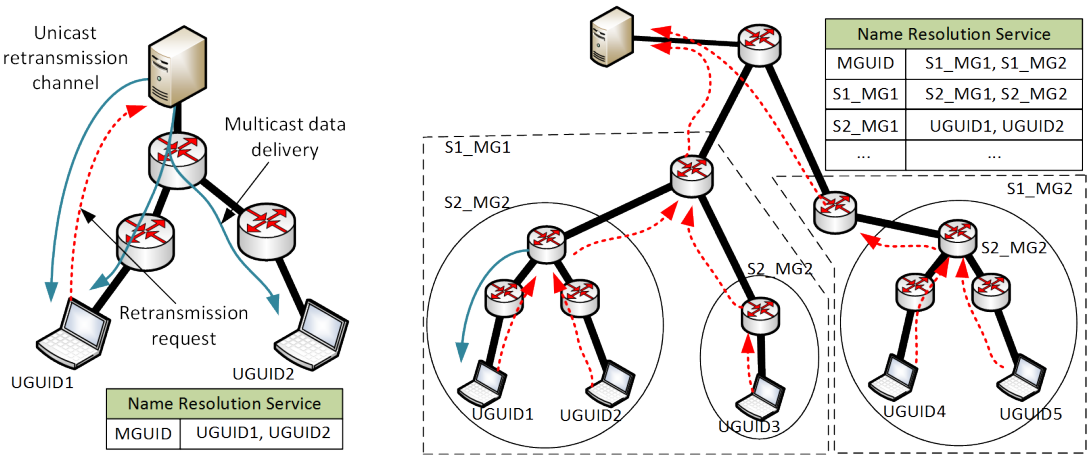

Figure 3.6: Multicast data delivery, small scale (left), large scale (right).

control.

Alleviating head-of-line blocking due to hop-by-hop transfer: A drawback inherent with hop-by-hop back pressure is the unfairness caused by head-of-line (HOL) blocking with FIFO queueing [47]. Theoretically, per-flow queuing solves this problem, but scheduling with per-flow queues is difficult to scale and is impractical with large numbers of flows. However, the in-network transport proxy provides some relief to this situation and alleviates the short-term unfairness. If a back-pressure signal is received for the chunk at the head of the sending queue, the transfers of chunks destined to other nodes will thus not be blocked because chunk at the head of the queue will be removed and pushed up to the transport proxy layer for temporary storage. The transport proxy will then attempt to transmit that chunk when the storage timer expires (or is dropped if the chunk is replaced in the storage buffer because of the replacement policy we described above).

3.3.5 Multicast

Multicast is naturally supported by name based architectures. For instance, in NDN, data is forwarded to the requestor based on the receipt of the corresponding request: each router forwards the data on the interface(s) the request for the data was received on. Multicast is thus fulfilled by the stateful forwarding plane [39]. In MobilityFirst, a

dynamically formed multicast group is explicitly identified by a globally unique identifier (GUID), which can be mapped into a set of individual clients' GUIDs or network addresses.

A small scale scenario is depicted on the left side of Figure 3.6. During the transmission the source of the multicast data marks outgoing chunks with a multicast service identifier and selects as destination GUID the one identifying the multicast group. Multicast clients send NACK messages over a unicast channel and the multicast source can identify which multicast group a specific client belongs to. Further, the source aggregates retransmission requests for the transmitted chunks; it can, either employ multicast again for retransmission when the number of requestors exceeds a threshold; otherwise retransmitted data chunks can be sent using unicast destination GUIDs that identify the specific nodes that need the retransmitted data.

As the number of participants increases we can exploit in-network transport proxies to build multiple levels of *multicast group GUID to a set of GUIDs* mappings recursively. This scenario is shown on the right side of Figure 3.6. In order to limit potential explosion of unfulfilled requests reaching the original source, transport proxies can be instructed through proper chunk marking, to discard retransmission requests that exceed a number of traversed proxies without encountering the missing chunks. In a scenario where reliability is not demanded, the source just use the *don't care* option of the reliability preference.

3.4 Implementation

Our implementation of MFTP consists of two parts: end-system transport operations that are implemented on the MobilityFirst client stack [41], and an in-network transport proxy implemented as a pluggable module inside a MobilityFirst Click router implementation.

Host Stack and API. The client host stack has been implemented on Linux as a user-level process built as an event-based data pipeline. Apart from the MF transport

protocol, the stack contains a name-based network layer and a reliable link layer with large chunk transfer. Applications interface with the host stack through socket APIs that are available as a linkable library and include the primitives *send, recv*, and *get*, and a set of meta-operations. Examples of meta-operations include those to bind or *attach* a GUID to one or more NAs. By specifying the options field in the API call, an application is able to configure transport parameters such as the i) desired chunk size; ii) end-to-end reliability preference; iii) NACK timeout; iv) willingness to use in-network proxy.

Router. The MobilityFirst software router is implemented as a set of routing and forwarding elements using Click [48]. The router implements MFTP transport proxy layer, MF network layer including intra-domain routing and dynamic binding using GNRS, and hop-by-hop reliable transfer. The transport layer (proxy) interacts with the intra-domain route look up component: if a lookup does not yield a valid next hop, the chunk is pushed up to the transport proxy. The transport proxy at the router will hold the data chunk for some time and attempt to rebind the name with one or more network addresses. When rebinding is successful, the chunk is pushed back down to the routing layer for forwarding.

Timers. There are three types of timers used in our implementation: one for triggering the transmission of an end-to-end NACK message, one for storage, and another one for link layer retransmission. For guaranteeing end-to-end reliability, timers are indispensable because a node has to learn about a remote node's failure impacting the end-end path. Previous experience with TCP end-to-end timers have taught us that timers need to be set loosely so as to reduce number of false alarms [49, 50], and not have a strict dependence of the transport protocol on timers for normal operations. In MFTP's design, this goal is achievable because: (i) different end-to-end service guarantees are dissected and each timer only handles a specific job; (ii) NACK timers and per-hop timers are associated with a chunk of data, rather than a single packet; (ii) the storage timer is only concerned about disconnection, and is thus decoupled from

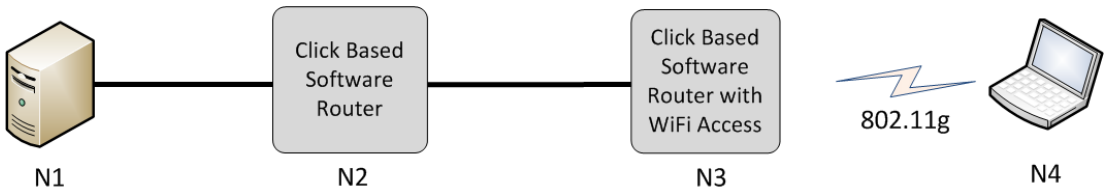

Figure 3.7: Experimental Setup

end-to-end latency and transferred data sizes, which could otherwise complicate timer settings.

3.5 Case studies and evaluations

In this section, we present how MFTP can be used in several different service scenarios, and quantitatively compare it with the performance of conventional HTTP and IP based protocols.

General experimental testbed setup. We use the ORBIT [51] wireless testbed for our experimental evaluation. Each machine in our experiment is equipped with Intel i7 2.93GHz processor and with 8GB RAM. In terms of networking capability, each node has one Gigabit-Ethernet interface and one WiFi interface with Atheros ath5k wireless driver. Physically all the nodes are connected to a single layer-2 switch; we use VLAN tags to create desired topology to isolate Ethernet traffic. For wireless traffic, we use 802.11g with the data rate fixed at 54Mbps. Access routers run hostapd [52] to operate as WiFi access points. We disable 802.11 authentication and use manual IP assignment (no DHCP), just to retain nearly the same amount of overhead with both MFTP and TCP for WiFi connection establishment. We considered a topology shown in Fig. 3.7, where a client, N_4 connects to a server N_1 through an access router N_3, which provides WiFi connectivity, and a regular router N_2.

Methodology. We evaluate three types of data delivery scenarios to compare MFTP with the current TCP/IP based architecture, in terms of the mechanisms employed, and

their performance. We emulate the end-to-end RTT's of local, coast-to-coast and inter-continental communications, use the emulation tool *netem* [53] to add 10ms, 50ms, 100ms RTT between the two routers, respectively. To emulate loss in a controlled manner, we again use *netem* to introduce 1% loss. With MF, we run the MF Click router prototype (mentioned in section 3.4), and a local GNRS server on both N_2 and N_3. The MF client stack runs on N_1 and N_4. For specific use cases, we run corresponding applications that interface with the client stack through the MF API. In the case of TCP-based experiments, we run Click IP routers on node N_2 and N_3. TCP segmentation offloading is turned off as the basic Click IP router drops TCP packets with size larger than 1500 bytes. We enabled manual Ethernet header encapsulation on the Click IP router so no ARP message is triggered during routing. On the two end nodes, the default version of TCP, TCP Cubic, is used. We configured both nodes' TCP receiver buffer to be 2MB, so that it is not a bottleneck in a high delay-bandwidth path in any of the experiments.

3.5.1 Large content delivery over wireless

We first look into a large volume data transfer experiment. A 400MB file is requested and transferred. A simple file retrieval application in MF is running on the two end nodes. In the case of TCP, we used iperf to generate a flow of equal size with the maximum packet payload size of 1400 bytes. We repeated this experiment for a number of network conditions: RTT being 10ms, 50ms, or 100ms, and loss on WiFi link being 0 or 1%, to explore their effect on both architectures' goodput (i.e., application throughput).

Fig. 3.8(a) shows the average throughput comparisons for the six different network settings. Both MFTP and TCP' throughputs are consistently high when there is no loss, despite varying the end-to-end latency. MFTP is slightly higher in throughput in the lossless cases. MFTP is significantly more robust in the presence of loss, e.g., the throughput degrades by only 10% when there is 1% residual loss, with all 3 RTT profiles. On the other hand, TCP throughput drops significantly when there is loss. For instance, with 50ms RTT, TCP throughput with loss drops to only a quarter of its

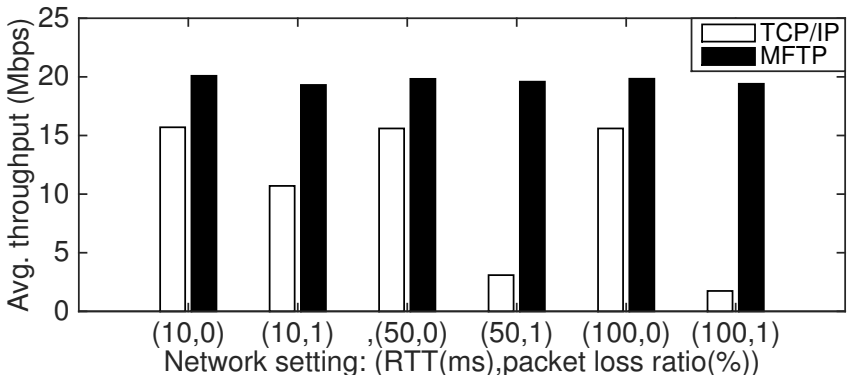

(a) Average throughput comparison for 6 different (RTT, loss rate) profiles.

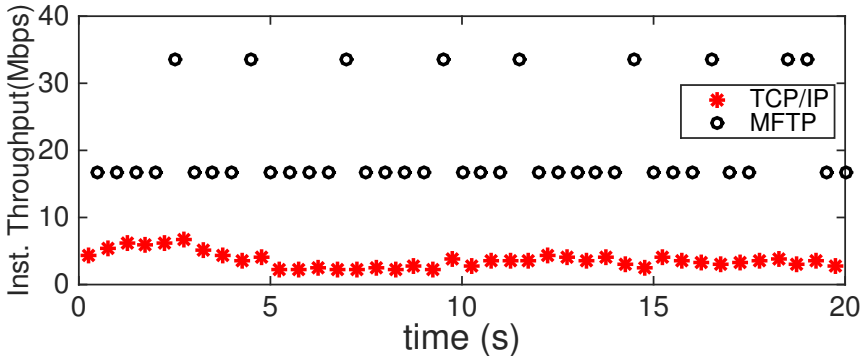

(b) Instantaneous throughput (per 500ms) for 50ms RTT and 1% loss.

Figure 3.8: Throughput comparison. MFTP is robust in the presence of loss.

throughput in the lossless case. Fig. 3.8(b) shows a plot of instantaneous throughput (averaged per 500ms) for 50ms latency and 1% loss. MF's PDU is a chunk of data, and in every 500ms, it receives at least one chunk (1MB), even in the presence of loss. With TCP, throughput fluctuate around 5Mbps. This is because the end-to-end congestion window is throttled whenever loss is detected. This misinterpretation of loss unrelated to congestion unnecessarily penalizes the flow. With MFTP, loss is not considered a signal for congestion, thus the sending rate is not throttled; moreover, loss happening at the last hop is recovered locally. Note in this experiment, the client suppresses the NACK messages because all the data has been successfully received.

3.5.2 Transport proxy for disconnection

We evaluate the benefits of using in-network transport proxies for handling client disconnections in content retrieval. We consider the same topology as above. The end-to-end RTT is set to be 50ms, and no loss is added so that difference in performance would not be incurred by having different mechanisms for error recovery. We use *netem* to introduce 100% loss intermittently, so as to emulate client disconnections. In the experiment, WiFi connectivity is on for 10 seconds; then is turned off for d seconds; then the connection is restored. During the first 10 seconds of connection, the client requests a 10MB file at a random time. The experiment is repeated 30 times for both MF and TCP. We compare the distribution of file retrieval response times between MFTP and TCP.

In Fig. 3.9(a), all the transfers having a response time of less than 10 seconds are completed before the disconnection. For the transfers that experience the disconnection, MFTP has at least 3 seconds lower response time (at 60th percentile). With 30 seconds disconnection, as shown in Fig. 3.9(b), the difference in response time is about 15 seconds at 70th percentile. It is worthwhile to understand the difference in the approaches taken by TCP and MFTP to dealing with disconnection. With TCP, the sender retransmits, based on a timer whose timeout value increases exponentially when the disconnection persists. In MFTP, the chunk in-transit is stored at the in-network proxy. A network address and next-hop lookup, rather than retransmission, is triggered when the storage timer for that chunk expires. Thus the transport proxy takes advantages of the global name resolution service in MF to learn whether there is a network address binding update for a client, and retransmits only when client is connected. This results in fewer retransmission attempts and more accuracy in the knowledge of end-to-end connectivity. Fig. 3.9(a) and Fig. 3.9(b) together suggest that MFTP's reduction in response time is nearly proportional to the length of the disconnection.

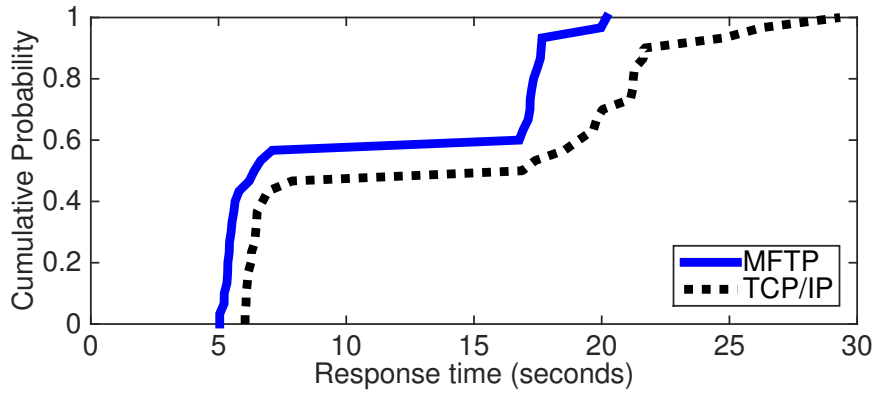

(a) With 10s disconnection

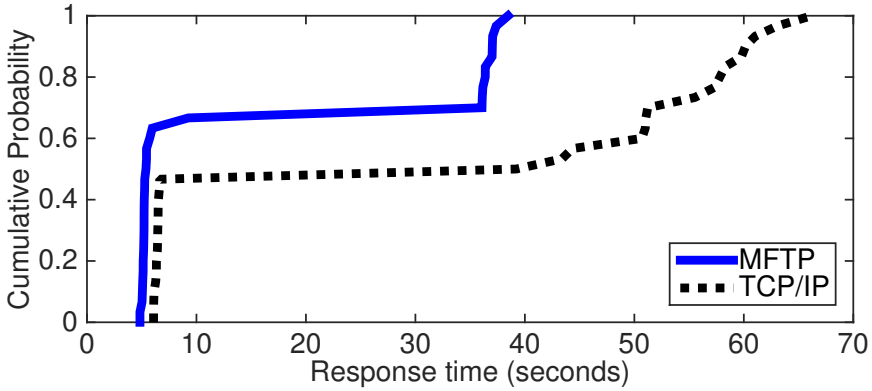

(b) With 30s disconnection

Figure 3.9: CDF of response times.

Comparison between network-proactive and receiver-driven approaches

We perform another set of experiments, with two different settings of proxy's storage and client's NACK timers. The network-proactive approach was used in the previous experiment, where the NACK timers are set conservatively, and thus clients rely on the network to re-deliver the data once a new connection is available. In the receiver-driven approach, the proxy does not re-initiate the delivery; the clients set the NACK timer aggressively and explicitly request retransmission, and the original server will request the retransmission from the transport proxy where the data is stored. As shown in

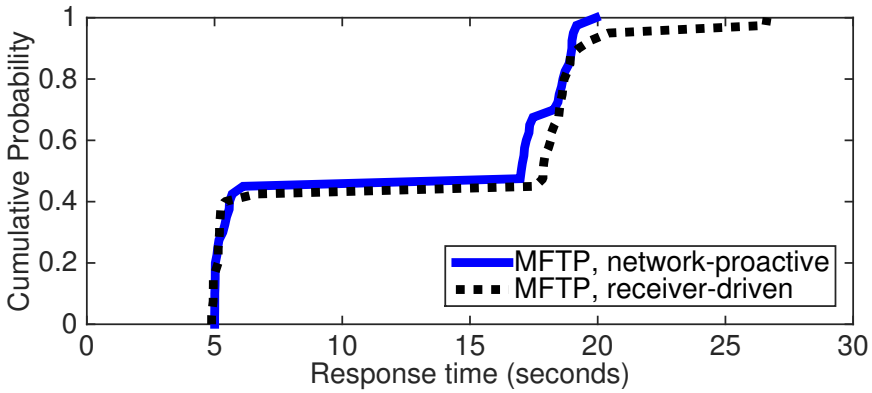

Figure 3.10: CDF of response times for network-proactive and receiver driven retransmissions, with 10s disconnection.

Fig. 3.10, similar to last set of experiments, half of the transfers complete without experiencing disconnection. The long tail for the receiver-driven curve corresponds to cases when a disconnection happens right after the client sends out the request. The content is transferred, but only a small portion gets delivered because client loses connectivity. The remaining data is temporarily stored at the proxy. The client has to wait for the NACK timeout to retrieve the data from the proxy. Thus, on the client side, whether it is an application or transport that is responsible to setting the end-to-end timer for a mobile client, a large number of characteristics, such as end-to-end path quality variations, disconnection interval, and content size, all collectively make estimating a reasonable timeout value difficult. On the other hand, retransmission from inside the network by the transport proxy only concerns itself with the connection/disconnection events. This improves performance, and more importantly, provides better manageability of end-to-end timers in mobile scenarios.

3.5.3 Web content retrieval

Web content retrieval is also evaluated. We use the same topology as described before to compare MFTP and TCP's performance. In addition to the routers, we run an Apache server (version 2.2.22) on node N_1, and a web browser emulator on node N_4 which

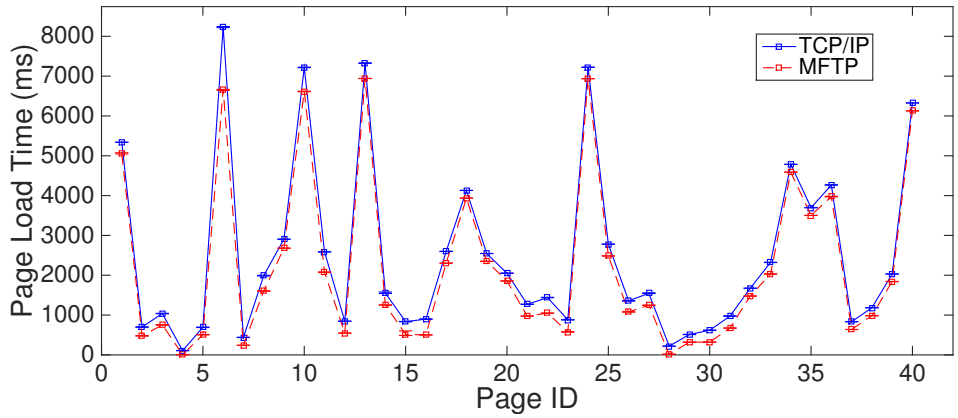

(a) 50ms RTT, no loss

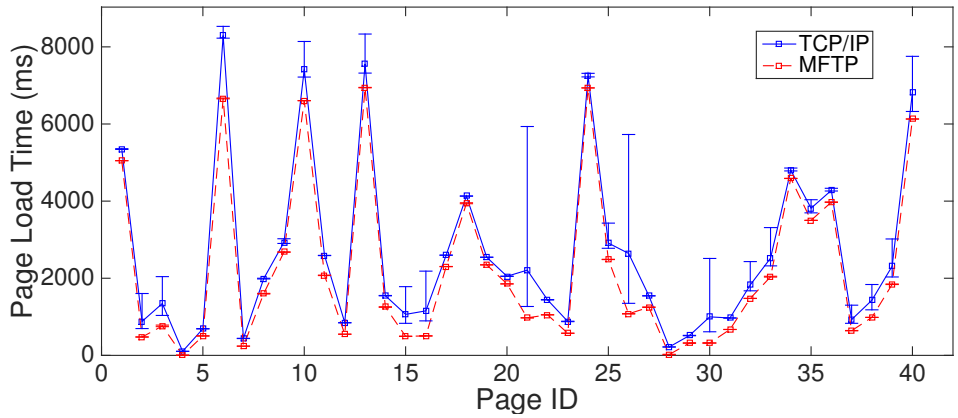

(b) 50ms RTT, 1% residual loss

Figure 3.11: Page Load Times (min, average, and max of 5 runs) for 40 different webpages.

requests webpages. We reuse the browser emulator, *epload*, presented in [54]. We also download the dataset introduced in [54] which consists of the real webpage objects of the 200 most accessed websites recorded by Alexa [55] in 2013. Among these we randomly select 40 pages and place them on N_1 to be hosted by the Apache server. In each run of the experiment, the browser emulator opens up 6 concurrent TCP connections (default settings in most browsers [54]) and sequentially request the 40 webpages. For experiments with MFTP, in order to keep the modifications at the application end-hosts to a minimum, we developed an MF-HTTP-MF proxy whose main job is translating

HTTP request and responses into MobilityFirst content requests and messages and vice-versa. We colocate 2 instances of these proxies with the HTTP components of the system, i.e., on the web client and on the server. For both MFTP and TCP, we performed 5 runs of the experiments with end-to-end RTT of 50ms, and 0 loss or 1% loss.

Fig. 3.11 are the plots for average page load times (PLT), i.e. the time between emitting the first HTTP request to reception of the last byte of last object, for the experiments with 50ms RTT. Page load time with MFTP is consistently lower than TCP. In the case of no loss, when there is a smaller amount of data to be transferred, e.g. page 21, 22, and 23, with TCP the PLT is about 30% higher than with MFTP. The difference in PLT can be attributed to several features of MFTP: (1) MFTP is connectionless, and thus there is no overhead due to setting up a connection; (2) TCP identifies different requested objects by differences in sequence numbers of that connection, while MFTP differentiates each requested object by a unique name, therefore HOL blocking (happens when multiple concurrent HTTP requests are fulfilled by a single TCP connection) does not occur with MFTP; (3) each TCP connection "slow-starts", whereas with MFTP, short transfers, such as retrieving web objects, are not subject to flow control and are regulated only by per-hop back-pressure based congestion control, which allows sender to transmit at full rate as long as no congestion signal. As can be seen in Fig. 3.11(b), loss introduces a great amount of variability with TCP. For instance, for page 21, the minimum PLT is around 1500ms with TCP, but the maximum is 6000ms, which is several orders of magnitude higher than with MFTP. For all the pages, MFTP maintains minimal variability in terms of page load time.

3.6 Related work

Future Internet architectures (FIA): A number of clean-slate information-centric network architecture designs [37,39,40,56] have been proposed recently to address challenges faced by today's IP network. They differ from each other in how they realize name-based service: while NDN [39] proposes a name-based routing approach in which

packets are forwarded directly based on name; some other architectures (like Mobility-First [37], XIA [40] and HIP [56]) place object names outside of the routing plane and uses a name resolution service to translate names to addresses.

Transport protocols for FIA: There have been a number of works on transport protocols for FIA, e.g. NDN [39], and XIA [40]. In NDN, a receiver asks for content by issuing a group of interest packets, i.e. requests; the corresponding data chunk is returned by the network in response to each interest. The NDN community has looked at how the transport layer can be adapted to such a interest-data interactive and multi-source/multi-path content-transfer pattern. Most of these works propose that the receiver maintains a Interest window and controls the issuing rate of interest packets (i.e., ICTP [57]), while others proposes a hop-by-hop Interest shaping scheme at each router (i.e., HR-ICP [58]). To support multi-source/multi-path transfer, CHoPCoP [59] proposes to utilize explicit congestion signaling from network to effectively notify the receiver about network conditions. In [60], a transport protocol, Tapa, for XIA architecture [40] is introduced which proposes to manage end-to-end delivery through segment-by-segment control. We share some of the techniques with these schemes here for the MFTP design. In addition, we investigate a broader set of ICN transport requirements which are derived from a collection of data delivery service scenarios. This allows MFTP to flexibly support different applications ranging from receiver-initiated retrieval, to sender-initiated publish, and from throughput-sensitive large file transfer, to latency-constrained short transfers of web objects.

Chapter 4

Scalable, network-assisted congestion control for the MobilityFirst future Internet architecture

4.1 Introduction

In this chapter, we present the design of a network-assisted congestion control framework for an Information Centric Network (ICN) architecture, MobilityFirst. Information Centric Network architectures place various intelligent functionalities inside the network to assist with efficient, and reliable data delivery. Unlike traditional congestion control in which only endpoints of the communication participate actively, the congestion control scheme to be presented involves active interaction between traffic sources and network routers, and depends heavily on various network functionalities offered by ICN.

Information/Content Centric Networks have been an area of significant research efforts in the recent past, with multiple proposed architectures ([38, 40, 61]) seeking to deliver information efficiently, based on a network layer that identifies content, independent of location. The network's ability to find better (and all) sources of content fully takes advantage of in-network caching, potentially reducing data retrieval latency by serving the data request from the cache which is closer to users compared with original servers. Several distinct features of ICN make traditional end-to-end congestion control such as TCP unsuitable. First, data transferred in ICN is often in large chunks, which means congestion detection and control has to operate on coarser granularity. Second, network may provide segment-wise or hop-by-hop reliability, to facilitate caching, or delay tolerant delivery, and to efficiently recover from loss locally. This results in infrequent end-to-end acknowledgements, which present challenges if congestion detection is

based upon such acknowledgements. In addition, as the network provides reliability at the protocol data unit (PDU) level, congestion control and reliability can be unbundled (as compared to TCP), potentially opening up to simpler congestion control schemes.

In this chapter, we present the design and evaluation of congestion control for one of the Information Centric Network architectures, MobilityFirst (MF) [38]. In MF, several of the intelligent network assistance mechanisms discussed above are considered core network functionality. MF routers are able to store content for caching as well as for delay tolerant delivery [62]. MF routers also provide reliability guarantees so that data can be transferred reliably along each hop, and efficiently over lossy links. These features make MF desirable for a variety of applications, one of which that is seeing growing interest is Internet-of-Things (IoT) networking. Under a very resource-constrained environment, endpoints in IoT systems, such as sensors, have limited power budget. Taking advantage of the network functionality we consider, such sensor nodes can implement a "send & forget" primitive to transfer data while conserving energy. Even though individual sensor traffic tends to be small and infrequent, for the the network to scale to tens of thousands of sensors, a flow and congestion control mechanism is highly desirable. Thus, being easy to scale is a major design goal for congestion management mechanisms in such IoT environments. In this chapter, we explore the role of network layer congestion control schemes for Information Centric Networks while also supporting the capability of end-systems to effectively use the "send & forget" primitive.

Network-layer congestion control mechanisms are not new. Previous work, which considers congestion control in networks with reliable links have proposed the use of "back pressure" to resolve congestion: when a queue is building up because of a higher arrival rate than the departure rate, a router seeks to stop incoming data from upstream nodes. Later when the queue occupancy drops, the upstream nodes are allowed to continue transmission to the router in question. Analysis showed that by allocating per-flow queues, such a back pressure based congestion control can achieve superior throughput and response times. For instance, [63] achieved this goal by limiting the per-flow queue length to be a single message. Nevertheless, maintaining per-flow state at

a router is costly. Modern routers can see millions of flows. Allocating and maintaining such a large number of queues requires multi-GB of high-speed memory, and scheduling with these queues introduces additional computational complexity and stringent latency requirements. The overall cost of per-flow queueing motivates us to pursue a different approach to congestion control than a simple back-pressure approach (see Fig. 4.1 for illustration of per-flow and per-interface queueing models).

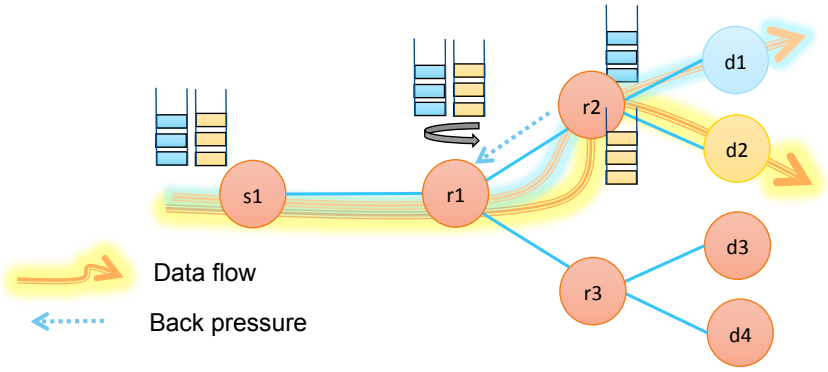

(a) Per-flow queueing: at node r1, each of the two flows which go through the same outgoing interface has its own queue, and r1 uses Round-Robin to schedule transfers from these queues.

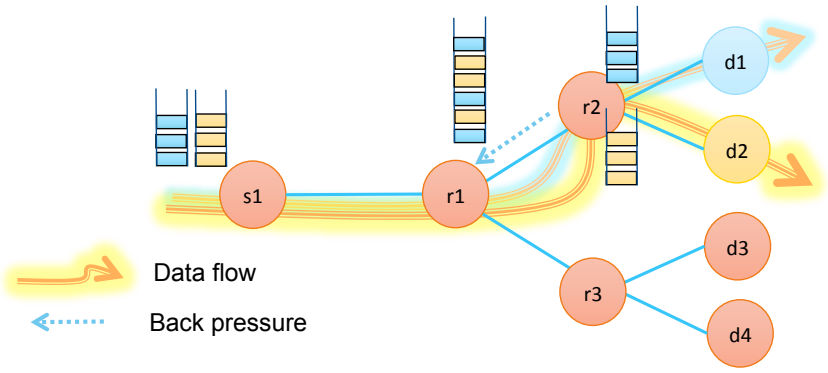

(b) Per-interface queueing: at r1, the data from two different flows residing in the same queue, based on the order they arrive. Note with back pressure, if the "blue" chunk experience congestion and blocks the transmission at r1, it delays the transmission of the subsequent "yellow" chunk.

Figure 4.1: Illustration of per-flow and per-if queueing

In this chapter, we design congestion control policies for the MobilityFirst architecture, with *per-interface queues*. We consider using rate control at traffic sources, in conjunction with router initiated explicit congestion notification. We show through simulation that our proposed scheme attains similar average link utilization to that of per-flow queueing based approaches. More importantly, our approach provides better fairness to competing flows, and can scale much more easily. The key contribution of this work lies in the lightweight, router-feedback based congestion control design which successfully manages congestion in a network with bulk data transfer. Even though the control loop feedback has less quantity and frequency, it is still able to sustain the network with high utilization and low queueing delay. Another important contribution is the demonstration of the feasibility of the per-interface queueing based approach. Per-interface queueing model aggregates multiple flows with the same outgoing interface into a single queue, and thus yields less computation and storage overhead. The improved efficiency and scalability are advantageous in practice.

In what follows, we first discuss several considerations for designing a congestion control algorithm for better performance. The detailed design, including the rate control algorithm and the explicit notification scheme, is presented in section 4.4. The proposed congestion control algorithms are evaluated using an event-driven simulator, and we present a broad range of simulation results in section 4.5. Section 4.6 discusses related works.

4.2 Background on MobilityFirst and data transport in MF

4.2.1 MobilityFirst architecture overview

MobilityFirst project [37, 38] presents a clean-slate Internet architecture that supports large-scale, efficient and robust network services with mobility as the norm. The MobilityFirst architecture is built upon a name-based service layer that serves as the "narrow-waist" of the protocol stack. The flat globally unique identifiers (GUIDs) are used at this layer to name all network-attached objects including hosts, content, services and even abstract context. The GUID works as the long-lasting identifier of an

object, and is decoupled from its network address(es). The Global Name Resolution Service (GNRS) exists to maintain GUIDs to network addresses mappings.

4.2.2 Data transport in MF

The design of data transport in MF contains three features:

Large chunk transfer The transport layer fragments the application data into large chunks, whose size can be negotiated by the two end-points based on a tradeoff between the overhead and the fair use of network resources across flows[1]. The chunk size is allowed to go up to the order of megabytes, to take advantage of high-bandwidth communication channels.

Hop-by-hop reliable transfer Each chunk is only forwarded once it has been received reliably in its entirety from the previous node. This reliability model is suitable for ICN, and MF in particular, due in part to the fact that the segment of data being transferred is named; moreover, ICN routers can have storage capability, and can temporarily store the in-transit copy to provide delay-tolerant delivery, and also cache a copy to serve future requests.

Lightweight end-to-end recovery Taking advantage of the hop-by-hop reliability of the network, the end-to-end mechanism is designed to be parsimonious and to have minimal overhead (important in mobile wireless environments) while primarily aiming to recover from node and link failures.

4.3 Design Considerations

In essence, congestion control aims to simultaneously optimize network performance along a number of frontiers: throughput, flow completion times, and fairness. The design of congestion control algorithms must take these aspects into consideration. We

[1] here a "flow" is identified by a (source GUID, destination GUID) pair.

discuss below three specific considerations on which our design of congestion control for achieving the above goal is based.

4.3.1 Back-pressure

There is an inherent problem when combining per-interface queuing with back-pressure: head-of-line blocking. An example is when a chunk at the head of the queue is blocked, all the subsequently queued chunks, possibly with different destinations, or even different next hop nodes (e. g. in a wireless ad hoc network) which are not experiencing congestion, will not be able to be transferred until the first chunk is pushed out. As a consequence, router utilization drops and overall network throughput could be impaired.

Admittedly, back-pressure cuts off traffic injection to the congested point, and stops the congestion from deteriorating. However, it only delays *traffic injection*, and does not change *composition* of traffic. It works to its full advantage with per-flow queueing, because fairness is acquired through scheduling, which is decoupled from queueing. With FIFO per-interface queueing, one needs to seek to use more proactive mechanisms to collectively and fairly injects traffic to the queue, and more proactively avoid congestion. Thus back pressure should only be used as a "fail safe" mechanism, so as to reduce incurred unfairness.

4.3.2 Fair share allocation

An important metric for evaluating congestion control mechanisms is fairness. A very common definition of fairness for flows sharing a single link is max-min fairness [64]. Max-min fairness is achieved if either all the requested rates are satisfied, or all the concurrent flows equally share the bandwidth. Lack of fairness can lead to conservative flows being penalized, or even starved.

Fairness across flows becomes even more important when network is reliable and flows are waiting at a single outgoing interface queue. Because in this case, congested flow can slow down the transmission or even block the interface, therefore hurt utilization. Fairness has to be built into the congestion control scheme to prevent this from

happening.

4.3.3 Router queue build-up

Queue occupancy is often an indication of congestion level. Queue buildup is a consequence of mismatch in input and output rate of the corresponding communication link, which leads to congestion. Fair rates allocation can resolve such mismatch. After that, however, even if the queue maintains a relatively stable occupancy, as a consequence of congestion, the queue may already be rather deep. Excessive queueing inside the network leads to higher end-to-end delay [65], even though flows may be fairly sharing the links. Congestion control should strive to regulate the input flows also to maintain a queue that is not overly deep.

Over-control can happen when the congestion control mechanisms overshoot, leading to queue being temporarily empty (queue underflow). Queue underflow results in the link sitting idle temporarily, and hurts utilization and throughput. Therefore over control is to be avoided.

4.4 Design

4.4.1 Overall framework

We consider each node has one or more outgoing network interfaces. Each interface connects the router to a neighboring node through certain communication medium, e.g. a fiber optical link, or a wireless channel. All traffic that need to be channeled through the same next hop will wait in the same outgoing interface FIFO queue. The unit of data that gets processed, i.e. queued, scheduled, etc, is *chunk*. A chunk is a fragmented portion of application data, and essentially a collection of packets that meet link layer PDU requirement. The traffic sources implement the Token Bucket algorithm to enforce any sending rate.

The general approaches considered here are source rate control with explicit notification from routers. The overall framework involves the following two major pieces (as illustrated in Fig. 4.2):

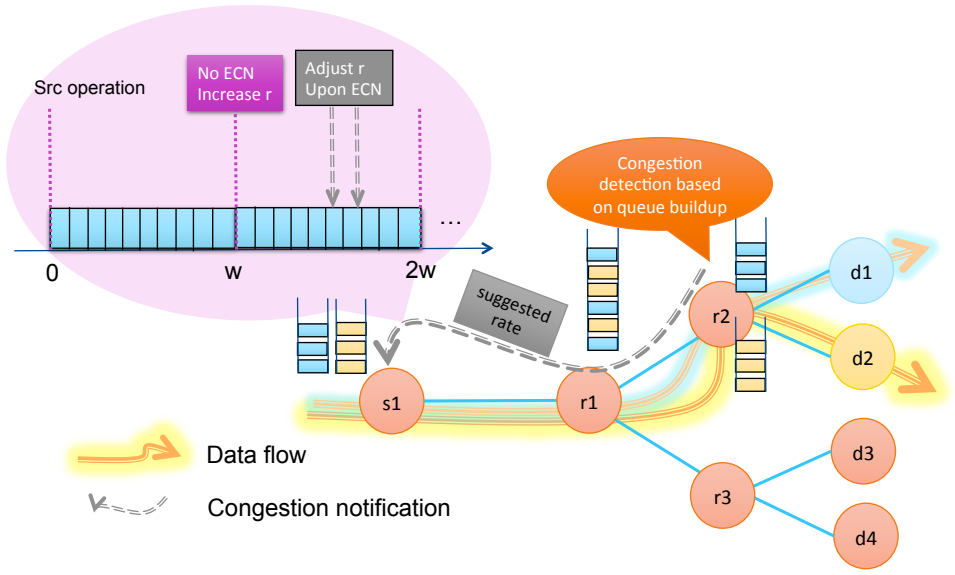

Figure 4.2: illustration of the congestion control framework

Router operation: if an incoming chunk sees the router's outgoing interface queue meets certain congestion criteria, the router computes a suggested rate for the chunk's traffic source, and sends a notification including that rate to the corresponding source node.

Source operation: If a congestion notification is received, the source synchronously reduces the rate if the suggested rate is lower than the current rate. On the other hand, for each W bytes of data sent, the source additively increases its sending rate if no congestion notification has been received.

4.4.2 Local fair share estimation

One of congestion control's goals is to let concurrent flows transmit at the rate matching its fair share of network bandwidth. This can be achieved either indirectly or directly. In most flavors of TCP, the traffic source detects congestion signals and reacts by multiplicatively reducing its rate. If the congestion persists, subsequent congestion signals will drive down the source rate further. Through the dynamism of source rate adjustment (usually constituting a sawtooth shape), the flow achieves its fair share as its average rate. Explicit notification based rate control facilitates a direct approach.

The routers can periodically estimate current fair share and notify each flow. Traffic sources cooperate by sending at the lowest rate reported among all en-route routers. Indeed, this approach has be applied, for instance, in ATM networks [64], and more recently in data center networks [66].

In our work, we also aim to achieve fair bandwidth allocation to concurrent flows, and we adjust the explicit notification based rate control framework to the specific challenges faced with a reliable network and bulk data transfer. We trade short-term allocation accuracy for feasibility of control over large units of data, and of less frequent feedbacks from routers.

On each link, the locally fair share of a flow is calculated as if this link is the bottleneck of the flow. Consider an outgoing interface with corresponding outgoing link of capacity C. We consider C to be max possible data rate the link can sustain. Letting $\hat{n}$ by the estimated number of concurrent flows, then we have the estimated fair share rate $C/\hat{n}$. How do we estimate $\hat{n}$? Currently we use transport layer sequence numbers to determine the start and end of a flow. Thus at any given time, the router is able to estimate how many flows are currently ongoing.

4.4.3 Rate adjustment

Frequency of control

Traffic sources need to reevaluate its sending rate periodically. We base the periodicity on a fixed number of bytes, W, so that the requirement on traffic destination feedback is relaxed (this can be done potentially with windowing). If there is no congestion notifications received during the transmission of W bytes of data, then the rate is increased by a fixed step size. On the other hand, the source reduces its rate synchronously upon receiving congestion notification.

Control logic

It may appear that if all the traffic sources adjust their rates based on the rate fair share computed by the routers, the router's input rate would converge to match the output

rate. However, in practice, a few factors introduce inaccuracies in applying this scheme. First, it takes time for the notification message to propagate to the corresponding traffic source. Depending on the latency from the router to the source, the traffic source essentially sends data at the "wrong" rate during the delivery of congestion notification message. The excessive amount of data contributes to further queue growth at the router. In addition, traffic dynamism happens at varied time scales, which leads to inaccuracy in the estimation of fair share rates. Apart from matching input rate to the output rate, router's queue length should be controlled so that queueing delay is reduced.

Thus the algorithm to be developed need to simultaneously accomplish several objectives: the sources are driven towards their fair share of bandwidth; meanwhile, queue length should be constrained to reduce queueing delay. Before describing the control logic, we need to first introduce a few notations. Consider an arbitrary traffic source, and an arbitrary router queue along the source's end-to-end path. Let R_{inc} be the additive rate increment of the source, and Q_{cap} be the queue capacity. The router generates a congestion notification if the observed queue length is greater than Q_{thresh}. We use R_0^m to denote the rate the source chooses to send at for the m-th block of W bytes of data, at the beginning of the m-th block. If no congestion notification is received during this transmission, the source maintains this rate for the entire block, and increases its rate additively at the beginning of the next block as following:

$$R_0^{m+1} = R_0^m + R_{\text{inc}} \tag{4.1}$$

The router computes a suggested rate for the incoming chunk, if current queue occupancy exceeds a threshold:

$$R_{k'}^m = R_{\text{fair}} - f(\frac{Q - Q_{\text{thresh}}}{Q_{\text{cap}}}) \cdot R_{\text{fair}} \tag{4.2}$$

where R_{fair} is the estimated local fair share at the router. We currently use a quadratic function to represent $f()$. The idea here is to reduce the rate more, if queue length is far beyond the desired queue occupancy. Upon obtaining this suggested rate through the notification message, the source evaluates and updates its rate if it is less than its

current rate:

$$R^m_{k+1} = \min\{R^m_k, R^m_{k'}\} \tag{4.3}$$

4.4.4 Aggressive bootstrapping

One way to bootstrap a rate control policy is to start at a low rate, and gradually increase the rate till the point when some router's queue overflows. The process of "polling" the appropriate sending rate can be shortened by using exponential growth, e. g. slow start in TCP. Nevertheless, it still takes several RTTs to reach at the equilibrium. Such a scheme i) renders lower utilization when the network is lightly loaded; ii) incurs extra latency that cannot be amortized easily.

Note that "slow start" mechanism is built on the premise that routers frequently and deliberately drops packets. Traffic sources take dropped packets as signals for congestion. However, there is no information or even a hint about the severity of congestion when a packet is dropped. In our scheme, such "hint" on the severity of congestion is passed to the traffic sources explicitly, based on which the sources can react more effectively. Furthermore, link layer back pressure strives to prevent congestion from worsening by stopping upstream routers from injecting more packets into downstream. As a consequence, packets drop is rare. The mechanics of explicit congestion notification and back pressure obviates the need for slow start; rather, the sources start "fast", and respond to congestion quickly and effectively.

4.5 Evaluation

4.5.1 Simulator

We built a chunk-level simulator for evaluating the proposed congestion control mechanisms. Links and nodes are modeled. All operations performed on the data, such as transmitting and receiving, are done on chunks, not packets. We implement both per-flow and per-interface queueing mechanisms, and their respective scheduling policies: Round Robin and FCFS, respectively. We also implement a module to perform congestion notification, and call it the Explicit Congestion Notification (ECN) module. Our

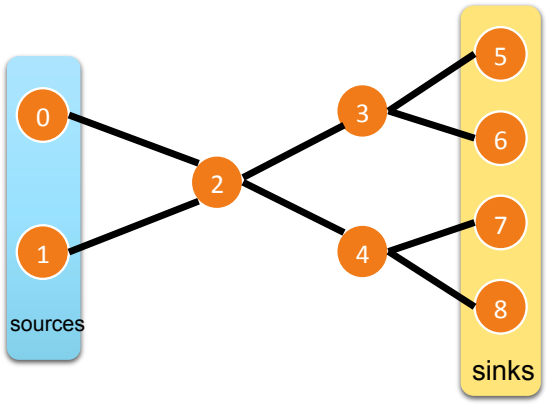

Figure 4.3: 9-node with single bottleneck topology

simulation evaluates how ECN can help improve network performance for per-interface queueing, and how close the performance of per-interface queueing with ECN is to that of per-flow queueing.

4.5.2 Single bottleneck scenario

We start by running the simulation with a 9-node, single-bottleneck network, as shown in Fig. 4.3. Each link in the network has a capacity of 54Mbps, and a latency of 1ms. Nodes 0 and 1 are the traffic sources, and nodes 5-8 are sinks. Each source node is sending data to each sink. We run the simulation with evenly distributed traffic, that is, the rate for each (source, sink) pair is the same and taking 12.5% of the overall network traffic demand (Table 1). We consider overall network throughput to be the sum of throughput achieved for each source, sink pair and plot it in Fig. 4.4(a). It can be seen from Fig. 4.4(a) that the three congestion management schemes perform equally well. A more interesting scenario is when the traffic in the network is skewed. For instance, with the traffic distribution specified in Table 2, the combined traffic towards sink node 8 is substantially higher than that towards any other sink. In this case, when the offered load increases beyond 10MB/s, PerIf cannot sustain the throughput as high as what the PerFlow policy achieves. However, when the proposed ECN mechanism is employed, the throughput is improved to match the 'optimal' throughput, as shown in the figure.

Source-sink pair	(0, 5-8), (1, 5-8)
Traffic percentage	12.5% each pair

Table 4.1: Even traffic distribution

Source-sink pair	(0, 5-7), (1, 5-7)	(0, 8), (1, 8)
Traffic percentage	$\frac{1}{12}$ each pair	$\frac{1}{4}$ each pair

Table 4.2: Skewed traffic distribution

Understanding cause of per-interface queueing throughput impairment

It is worthwhile to understand the cause of throughput impairment due to per interface queueing, and the reason why explicit congestion notification based control is complementary to such queueing discipline. To this end, we need to take a look at throughput by traffic sinks, when the traffic is skewed. Fig. 4.5(a) corresponds to the simulation with offered load being 0.7MB/s, and all the three mechanisms yield the same throughput, despite network traffic is skewed. Because at this time, the aggregated traffic demand is still well under the network's capacity. Fig. 4.5(b) shows the throughput by sink for an offered load of 1.1MB/s, which brings congestion. It can be seen that PerFlow queueing based mechanism improves overall network throughput by suppressing the overly high demand of sink node 8. With PerIf queueing, traffic distribution is not altered: traffic to sink node 8 is three times of any other sink node. This is because when there is congestion at a queue, the transmission of the data chunk at the head of the queue is delayed, and so are all the chunks behind the head. During the blockage, the queue is sitting idle, without any data being transmitted. Thus this 'back pressure' mechanism resulted in poor link utilization in such cases. Evidently, ECN helps bring more balanced traffic allotment to PerIf queueing systems, as shown in Fig. 4.5.

4.5.3 RocketFuel topologies

We next run the simulations on a number of network topologies provided in the RocketFuel dataset, including Abilene, Exodus and Sprint. We report here the results for

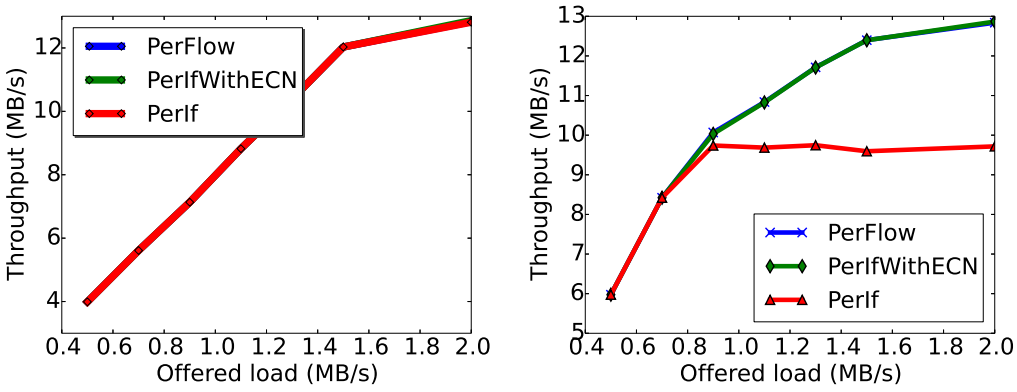

(a) evenly distributed traffic

(b) skewed traffic

Figure 4.4: Overall network throughput

the Abilene network, as this topology consists of multiple bottlenecks and generates results that are quite representative of all the topologies. The Abilene network consists of 16 nodes and is shown in Fig. 4.6. We consider each node i generates traffic to every other node in the network, and all the (source, sink) pairs have the same amount of offered load.

Mean link utilization One of the primary goals of congestion control is to enable the network to operate with high utilization. Fig. 4.7 shows the mean link utilization of the 22 links, for offered load values from 0.35MB/s to 9MB/s. We can see that per-flow queueing achieves the highest mean link utilization consistently. Per interface queueing without ECN performs rather poorly. However, with ECN, per-interface queueing achieves more than 2 orders of magnitude of throughput improvement. Also, its curve flattens out at around 0.93, which is about 6% lower than that of per-flow queueing. Note that in practice networks are operating below saturation, where PerIfWithECN has identical link utilization with PerFlow's.

Throughput by (source, sink) pairs We then turn our attention from network level aggregates to individual source and sink pairs' measurements. Fig. 4.8 shows the CDF plots for throughputs across all (source, sink) pairs. It can be seen that with PerIf

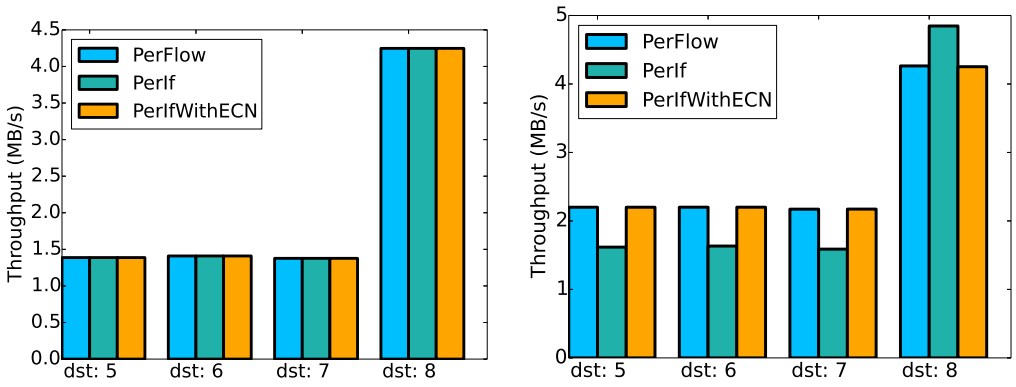

(a) offered load 0.7MB/s

(b) offered load 1.1MB/s

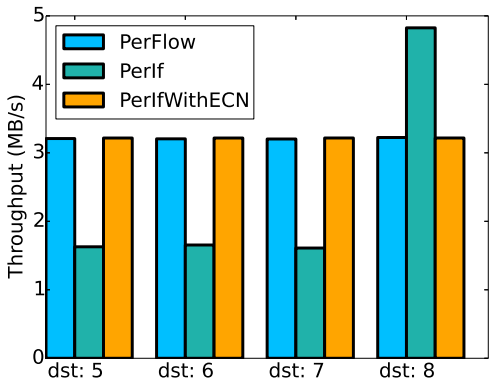

(c) offered load 2.0MB/s

Figure 4.5: Throughput by traffic sink, with skewed traffic

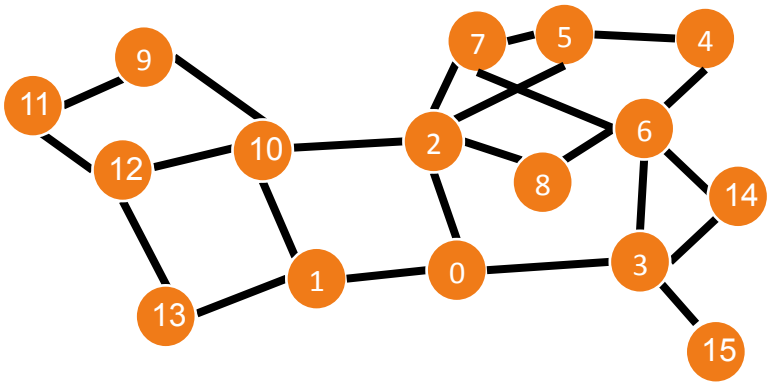

Figure 4.6: Abilene network topology

queueing, nearly 80% of the source-sink have a throughput of under 0.05. From the plot,

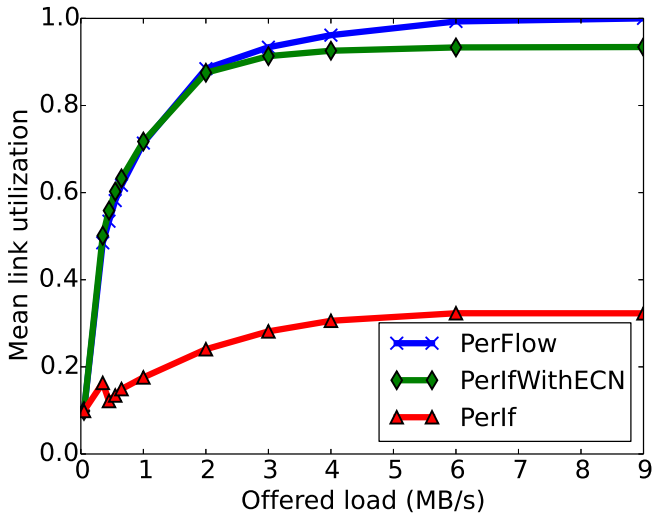

Figure 4.7: Mean link utilization

both PerFlow and PerIfWithECN perform significantly better than PerIf. With PerFlow, more than 70% source sink pairs obtain greater than .30MB/s throughput. With PerIfWithECN, around 50% do; nevertheless, the minimum throughput is 0.19MB/s, whereas PerFlow's minimum is around 0.01MB/s. Therefore, PerIfWithECN substantially reduces the disparity between the min and max throughput.

Using the same data, Fig. 4.8(b) plots the histogram of throughput, with 0.01MB/s bins. In light of the histogram, it is easier to see the differences in the distribution pattern. The smallest 30% throughput values are spread across the 0.01MB/s to 0.33MB/s range. This is because PerFlow reacts to all the congested queues along the path and consequently, the flow with a longer path is more likely to suffer from low throughput. For PerIfWithECN, the throughput distribution are divided into 3 clusters: about 50% is around 0.38MB/s, 20% around 0.24MB/s, and the remaining 30% around 0.20MB/s, as a result of only reacting to the most congested bottleneck along the path. This allows it to improve the minimum throughput and achieve better fairness.

Fairness index The source-sink pair throughput distribution presented above has significant implication on the fairness achieved by each congestion management mechanism. We evaluate different schemes' fairness using hop weighted Jain's fairness index

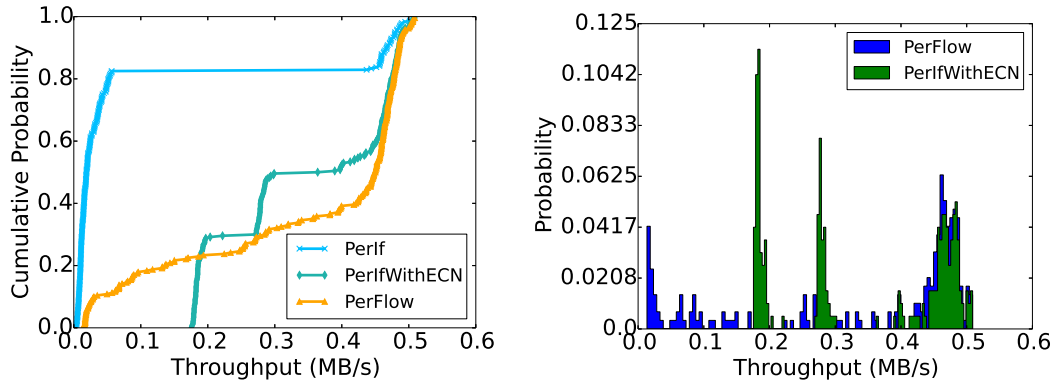

(a) CDF of throughput of all (source, sink) pairs (b) Histogram of throughput of all (source, sink) pairs

Figure 4.8: Throughput across (source, sink) pairs

(JFI). Suppose there are n flows and each flow i has throughput x_i and hop count h_i. The hop-weighted fairness index is given by:

$$I = \frac{(\sum_{i=1}^{n} x_i \cdot h_i)^2}{n \sum_{i=1}^{n} (x_i \cdot h_i)^2} \tag{4.4}$$

The results shown in Fig. 4.9 suggest, under congestion, i.e. for all the offered load >0.05MB/s, that per-interface queueing with ECN significantly improve throughput fairness. The improved fairness can be partially attributed to the fact that per-interface queueing with ECN improves the lowest (source, sink) throughputs.

Chunk transfer response time In addition to throughput, we also evaluate delay in the data transfers. Since the data transfer is done in chunks, we can easily evaluate the time it takes to transfer a chunk from the source to the sink. We call it chunk transfer response time. In the plot, the boxes (barely shown) represent 1st to 3rd quartile, and each whisker above the box represents an outlier that is above 90th percentile. As seen in Fig. 4.10, when there is no congestion (offered load being 0.05MB/s), response time distributions are roughly the same across. However, when offered load is greater, PerFlow based scheme introduces substantially greater delay, compared with PerIfWithECN.

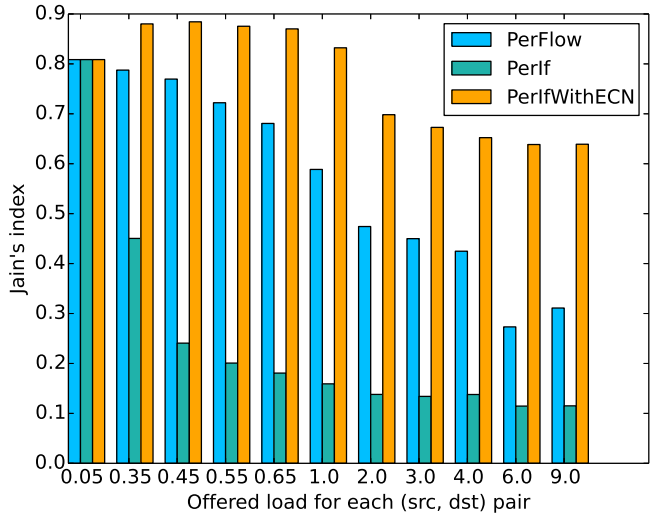

Figure 4.9: Hop-weighted Jain's fairness index

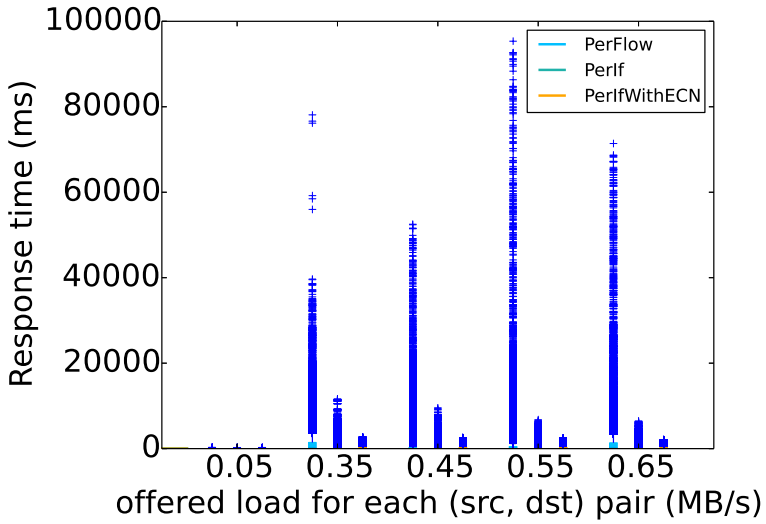

Figure 4.10: Chunk transfer response times

4.6 Related work

Back pressure: [67] laid the theoretical foundation for back pressure based congestion control for networks with reliable links. It considered each node maintained per-destination queues, and introduced a scheduling policy for maximizing network throughput. The scheduling policy can be summarized as, at each interval, letting each

node schedule to transfer the data in one queue whose length has the max difference against its next hop's queue. [63] followed the same idea, and considered each node maintaining per flow queues. In [63], each per-flow queue has certain capacity. Once the capacity is reached, that flow is considered to generate back pressure, i.e. the node will not be able to accept more data for that flow. When scheduling, the flow to be transferred is selected in a Round Robin fashion among all flows that are not experiencing back pressure. [63] showed through experimental validation that it achieved substantially better throughput and fairness compared with TCP. Nevertheless, the scalability concern arising from keeping per-flow queues was not addressed.

Explicit congestion notification based congestion control: The idea of using explicit congestion notification dates back to several decades ago, for instance, [68] considered using a single bit to indicate congestion. In [69], a source to destination flow explicitly requests certain rate with which the flow deadline can be met. Then if the requested rate can be satisfied, each on-path router exposes its allocated rate for the next interval. Otherwise the source has to wait and re-request rate in the future. Therefore the source relies on constant rate share updates from routers. Our work is different from existing ones mainly in the frequency the notification is sent.

Chapter 5

Concluding remarks

As wireless Internet usage gradually becomes the most popular way of accessing the Internet, it is crucial to engineer new solutions to overcome the challenges presented by wireless/mobile data delivery. This dissertation proposes algorithmic and protocol designs to address three problems: multicast, reliable data transport, and congestion control.

We first investigated integrated resource allocation for wireless networks which employ random network coding as the transport scheme. We used a differential equation based framework that models RNC throughput, thereby enabling the analysis of RNC performance in terms of PHY and MAC layer parameters. Using this framework, we designed dynamic power control and CSMA mean backoff delay control algorithms to improve the performance of RNC. Specifically, we used gradient based resource allocation algorithms and evaluated both centralized and online versions of them, via the use of differential equation solvers and event driven simulations. Our results revealed that such network coding aware resource allocation significantly improves the throughput of destination nodes in RNC. We also observed that such integrated power control can regain the broadcast advantage. Beyond the use cases of power control and CSMA backoff control, the framework and approach presented in this dissertation can be generally applied to joint power and CSMA backoff control as well as a variety of resource allocation problems for RNC.

We then presented the design of a clean-slate transport layer protocol for the MobilityFirst future Internet architecture. The proposed transport layer protocol, called MFTP, is based on an understanding of the key requirements of name-based Information Centric Networks. These requirements include the use of names rather than

addresses for routing, in-network storage, hop-by-hop reliability and multicasting as a basic service. Several core transport protocol components responsive to the above requirements were identified and discussed in the context of the MobilityFirst protocol stack. A proof-of-concept experimental validation has been developed and used to demonstrate feasibility and significantly improved performance relative to conventional TCP/IP for several use cases including large file transfer, web access and late binding/delay tolerant services. The reported results represent an initial design of MFTP to enable services on the MobilityFirst network. The protocol is expected to evolve with ongoing experimental evaluations and prototype GENI deployment.

Finally, we designed a network-layer congestion control scheme to support efficient data delivery at scale in the information-centric MobilityFirst network architecture. The proposed scheme utilizes router's explicit congestion notifications as feedback for source rate control, operating on bulk data transfer and with less frequent control looping. Along with its simple per-interface queueing mechanism which is easy to scale, the scheme is distinct from per-flow queueing based scheme. Compared with existing per-flow based network-layer congestion control scheme, the proposed congestion control is shown through simulation to be able to improve bulk data transfer delay, fairness across flows and better scalability, at an acceptable cost of only less than 6% average link utilization degradation under link saturation. This design fills a critical missing piece in the MF architecture to efficiently support IoT networking at scale.

References

[1] J. Tang, G. Xue, C. Chandler, and W. Zhang, "Link scheduling with power control for throughput enhancement in multihop wireless networks," *in IEEE Transactions on Vehicular Technology*, vol. 55, no. 3, pp. 733 – 742, May 2012.

[2] L. Georgiadis, M. Neely, and L. Tassiulas, "Resource allocation and cross-layer control in wireless networks," *Foundations and Trends® in Networking*, vol. 1, no. 1, 2006.

[3] X. Lin, N. Shroff, and R. Srikant, "A tutorial on cross-layer optimization in wireless networks," *Selected Areas in Communications, IEEE Journal on*, vol. 24, no. 8, pp. 1452 –1463, aug. 2006.

[4] M. Chiang, S. Low, A. Calderbank, and J. Doyle, "Layering as optimization decomposition: A mathematical theory of network architectures," *Proceedings of the IEEE*, vol. 95, no. 1, pp. 255 –312, jan. 2007.

[5] R. Ahlswede, N. Cai, S.-Y. Li, and R. Yeung, "Network information flow," *IEEE Transactions on Information Theory*, vol. 46, no. 4, pp. 1204 –1216, July 2000.

[6] K. Han, T. Ho, R. Koetter, M. Medard, and F. Zhao, "On network coding for security," *IEEE Military Communications Conference (MILCOM)*, pp. 1 – 6, Oct. 2007.

[7] A. Dimakis, P. Godfrey, Y. Wu, M. Wainwright, and K. Ramchandran, "Network coding for distributed storage systems," *Information Theory, IEEE Transactions on*, vol. 56, no. 9, pp. 4539 –4551, sept. 2010.

[8] C. Gkantsidis and P. Rodriguez, "Network coding for large scale content distribution," in *INFOCOM 2005. 24th Annual Joint Conference of the IEEE Computer and Communications Societies. Proceedings IEEE*, vol. 4, march 2005, pp. 2235 – 2245 vol. 4.

[9] D. Lun, N. Ratnakar, M. Medard, R. Koetter, D. Karger, T. Ho, E. Ahmed, and F. Zhao, "Minimum-cost multicast over coded packet networks," *Information Theory, IEEE Transactions on*, vol. 52, no. 6, pp. 2608–2623, 2006.

[10] Y. Xi and E. Yeh, "Distributed algorithms for minimum cost multicast with network coding," *Networking, IEEE/ACM Transactions on*, vol. 18, no. 2, pp. 379–392, 2010.

[11] K. Rajawat, N. Gatsis, and G. Giannakis, "Cross-layer designs in coded wireless fading networks with multicast," *Networking, IEEE/ACM Transactions on*, vol. 19, no. 5, pp. 1276–1289, 2011.

[12] D. Traskov, D. S. Lun, R. Koetter, and M. Medard, "Network coding in wireless networks with random access," in *Information Theory, 2007. ISIT 2007. IEEE International Symposium on*, june 2007, pp. 2726 –2730.

[13] D. Zhang, K. Su, and N. B. Mandayam, "Network coding aware resource allocation to improve throughput," *IEEE International Symposium on Information Theory (ISIT)*, 2012.

[14] T. Ho, R. Koetter, M. Medard, D. Karger, and M. Effros, "The benefits of coding over routing in a randomized setting," *in IEEE International Symposium on Information Theory*, p. 442, Jul. 2003.

[15] D. Zhang and N. B. Mandayam, "Analyzing random network coding with differential equations and differential inclusions," *IEEE Transactions on Information Theory*, vol. 57, no. 12, pp. 7932–7949, Dec. 2011.

[16] D. Zhang, N. Mandayam, and S. Parekh, "DEDI: A framework for analyzing rank evolution of random network coding in a wireless network," in *Information Theory Proceedings (ISIT), 2010 IEEE International Symposium on*, june 2010, pp. 1883 –1887.

[17] A. Ruszczynski, *Nonlinear Optimization*. Princeton University Press, 2006.

[18] M. Chiang, P. Hande, T. Lan, and C. Tan, "Power control in wireless cellular networks," *Foundations and Trends® in Networking*, vol. 2, no. 4, April 2008.

[19] G. Foschini and Z. Miljanic, "A simple distributed autonomous power control algorithm and its convergence," *Vehicular Technology, IEEE Transactions on*, vol. 42, no. 4, pp. 641 –646, nov 1993.

[20] R. Yates, "A framework for uplink power control in cellular radio systems," *Selected Areas in Communications, IEEE Journal on*, vol. 13, no. 7, pp. 1341 –1347, sep 1995.

[21] J. Zander, "Distributed cochannel interference control in cellular radio systems," *Vehicular Technology, IEEE Transactions on*, vol. 41, no. 3, pp. 305 –311, aug 1992.

[22] M. Chiang and J. Bell, "Balancing supply and demand of bandwidth in wireless cellular networks: utility maximization over powers and rates," in *INFOCOM 2004. Twenty-third AnnualJoint Conference of the IEEE Computer and Communications Societies*, vol. 4, march 2004, pp. 2800 – 2811 vol.4.

[23] P. Hande, S. Rangan, M. Chiang, and X. Wu, "Distributed uplink power control for optimal sir assignment in cellular data networks," *Networking, IEEE/ACM Transactions on*, vol. 16, no. 6, pp. 1420 –1433, dec. 2008.

[24] C. Saraydar, N. Mandayam, and D. Goodman, "Efficient power control via pricing in wireless data networks," *Communications, IEEE Transactions on*, vol. 50, no. 2, pp. 291 –303, feb 2002.

[25] K. Su, D. Zhang, and N. B. Mandayam, "Network coding aware power control in wireless netoworks," *in 46th Annual Conference on Information Sciences and Systems (CISS)*, 2012.

[26] C. G. Broyden, "A class of methods for solving nonlinear simultaneous equations," *Mathematics of Computation (American Mathematical Society)*, Oct. 1965.

[27] "Propagation data and prediction methods for the planning of indoor radio communication systems and the radio local area networks in the frequency range 900 mhz to 100 ghz," *ITU-R Recommendations*, 2001.

[28] J. Nocedal and S. J. Wright, *Numerical Optimization.* Springer., 2006.

[29] L. Jiang and J. Walrand, "A distributed csma algorithm for throughput and utility maximization in wireless networks," *Networking, IEEE/ACM Transactions on*, vol. 18, no. 3, pp. 960 –972, june 2010.

[30] ——, "Approaching throughput-optimality in distributed csma scheduling algorithms with collisions," *Networking, IEEE/ACM Transactions on*, vol. 19, no. 3, pp. 816 –829, june 2011.

[31] J. Ni and R. Srikant, "Distributed csma/ca algorithms for achieving maximum throughput in wireless networks," in *Information Theory and Applications Workshop, 2009*, feb. 2009, p. 250.

[32] R. Boorstyn, A. Kershenbaum, B. Maglaris, and V. Sahin, "Throughput analysis in multihop csma packet radio networks," *Communications, IEEE Transactions on*, vol. 35, no. 3, pp. 267 – 274, mar 1987.

[33] S. C. Liew, C. H. Kai, H. C. Leung, and P. Wong, "Back-of-the-envelope computation of throughput distributions in csma wireless networks," *Mobile Computing, IEEE Transactions on*, vol. 9, no. 9, pp. 1319 –1331, sept. 2010.

[34] J. H. Saltzer, D. P. Reed, and D. D. Clark, "End-to-end arguments in system design," *ACM TOCS*, 1984.

[35] B. Ahlgren and et Al, "Design considerations for a network of information," in *ACM CoNEXT*, 2008.

[36] A. Ghodsi, S. Shenker, T. Koponen, A. Singla, B. Raghavan, and J. Wilcox, "Information-centric networking: Seeing the forest for the trees," in *ACM HotNets.* ACM, 2011.

[37] MobilityFirst Project, http://mobilityfirst.winlab.rutgers.edu/.

[38] D. Raychaudhuri, K. Nagaraja, and A. Venkataramani, "Mobilityfirst: a robust and trustworthy mobility-centric architecture for the future internet," *ACM SIGMOBILE Mobile Computing and Communications Review*, 2012.

[39] V. Jacobson *et al.*, "Networking named content," in *ACM CoNEXT.* ACM, 2009.

[40] D. Han, A. Anand, F. R. Dogar, and Others, "Xia: Efficient support for evolvable internetworking." in *USENIX NSDI*, 2012.

[41] F. Bronzino, K. Nagaraja, I. Seskar, and D. Raychaudhuri, "Network service abstractions for a mobility-centric future internet architecture," in *ACM MobiArch*. ACM, 2013.

[42] A. Erramilli and R. P. Singh, "A reliable and efficient multicast for broadband broadcast networks," in *ACM Workshop on Frontiers in Computer Communications Technology*, 1988.

[43] S. C. Nelson, G. Bhanage, and D. Raychaudhuri, "Gstar: Generalized storage-aware routing for mobilityfirst in the future mobile internet," in *ACM MobiArch*. ACM, 2011.

[44] T. Vu and Others, "Dmap: A shared hosting scheme for dynamic identifier to locator mappings in the global internet," in *IEEE ICDCS*, June 2012.

[45] A. Sharma, X. Tie, H. Uppal, A. Venkataramani, D. Westbrook, and A. Yadav, "A global name service for a highly mobile internetwork," in *ACM SIGCOMM*, 2014.

[46] S. Mukherjee, K. Su, N. B. Mandayam, K. Ramakrishnan, D. Raychaudhuri, and I. Seskar, "Evaluating opportunistic delivery of large content with tcp over wifi in i2v communication," *IEEE LANMAN*, 2014.

[47] M. Gerla and L. Kleinrock, "Flow control: A comparative survey," *IEEE Transactions on Communications*, 1980.

[48] E. Kohler and et al, "The click modular router," *ACM Transactions on Computer Systems*, 2000.

[49] L. Zhang, "Why tcp timers don't work well," in *ACM SIGCOMM*, 1986.

[50] I. Psaras and V. Tsaoussidis, "Why tcp timers (still) don't work well," *Computer Networks*, 2007.

[51] ORBIT testbed, http://www.orbit-lab.org/.

[52] hostapd, http://wireless.kernel.org/en/users/Documentation/hostapd.

[53] netem: network emulation tool, http://www.linuxfoundation.org/collaborate/workgroups/networking/netem.

[54] X. S. Wang, A. Balasubramanian, A. Krishnamurthy, and D. Wetherall, "How speedy is spdy," in *USENIX NSDI*, 2014.

[55] Alexa: the top 500 sites on the web, http://www.alexa.com/topsites.

[56] R. Moskowitz, P. Nikander, P. Jokela, and T. Henderson, "Host identity protocol," *RFC 5201, April*, 2008.

[57] S. Salsano and et Al, "Transport-layer issues in information centric networks," in *ACM ICN*, 2012.

[58] G. Carofiglio, M. Gallo, and L. Muscariello, "Joint hop-by-hop and receiver-friven interest control protocol for content-centric networks," in *ACM ICN*, 2012.

[59] F. Zhang, Y. Zhang, A. Reznik, H. Liu, C. Qian, and C. Xu, "A transport protocol for content-centric networking with explicit congestion control," in *IEEE ICCCN*, 2014.

[60] F. R. Dogar and P. Steenkiste, "Architecting for edge diversity: Supporting rich services over an unbundled transport," in *CoNEXT*, 2012.

[61] L. Zhang *et al.*, "Named data networking," *SIGCOMM CCR*, 2014.

[62] K. Su *et al.*, "Mftp: A clean-slate transport protocol for the information centric mobilityfirst network," in *ACM ICN*, 2015.

[63] M. Li, D. Agrawal, D. Ganesan, and A. Venkataramani, "Block-switched networks: A new paradigm for wireless transport," in *USENIX NSDI*, 2009.

[64] L. Kalampoukas, A. Varma, and K. K. Ramakrishnan, "An efficient rate allocation algorithm for atm networks providing max-min fairness," in *Proceedings of the IFIP Sixth International Conference on High Performance Networking VI*, 1995.

[65] J. Gettys, "Bufferbloat: Dark buffers in the internet," *IEEE Internet Computing*, vol. 15, no. 3, pp. 96, 95, 2011.

[66] M. Alizadeh, A. Greenberg, D. A. Maltz, J. Padhye, P. Patel, B. Prabhakar, S. Sengupta, and M. Sridharan, "Data center tcp (dctcp)," in *SIGCOMM '10*, 2010.

[67] L. Tassiulas and A. Ephremides, "Stability properties of constrained queueing systems and scheduling policies for maximum throughput in multihop radio networks," *Automatic Control, IEEE Transactions on*, vol. 37, no. 12, pp. 1936–1948, Dec 1992.

[68] K. K. Ramakrishnan and R. Jain, "A binary feedback scheme for congestion avoidance in computer networks with a connectionless network layer," *SIGCOMM Comput. Commun. Rev.*, vol. 18, no. 4, Aug. 1988.

[69] C. Wilson, H. Ballani, T. Karagiannis, and A. Rowtron, "Better never than late: Meeting deadlines in datacenter networks," *SIGCOMM Comput. Commun. Rev.*